1	
2	Switching Neuron Contributions to Second Network Activity
3	
4	
5	Savanna-Rae H Fahoum
6	Dawn M Blitz
7	
8	Department of Biology and Center for Neuroscience
9	Miami University
10	Oxford OH 45056
11	
12	Running title: Switching Neuron Contributions to Second Network
13	
14	¹ Corresponding Author:
15	Dawn M. Blitz
16	700 E High St
17	PSN 212
18	Oxford OH, 45056
19	blitzdm@miamoh.edu
20	513-529-6327
21	
22	ORCiD: 0000-0002-1281-6010
23	
24	
25	
26	
27	
28	
29	

Abstract

30

31

32

33

34

35

36

37

38

39

40

41

42

43

44

45

46

47

48

49

50

51

52

Network flexibility is important for adaptable behaviors. This includes neuronal switching, where neurons alter their network participation, including changing from single- to dual-network activity. Understanding the implications of neuronal switching requires determining how a switching neuron interacts with each of its networks. Here, we tested 1) whether "home" and second networks, operating via divergent rhythm generation mechanisms, regulate a switching neuron, and 2) if a switching neuron, recruited via modulation of intrinsic properties, contributes to rhythm or pattern generation in a new network. Small, well-characterized feeding-related networks (pyloric, ~1 Hz; gastric mill, ~0.1 Hz) and identified modulatory inputs make the isolated crab (Cancer borealis) stomatogastric nervous system (STNS) a useful model to study neuronal switching. In particular, the neuropeptide Gly¹-SIFamide switches the lateral posterior gastric (LPG) neuron (2 copies) from pyloric-only to dual-frequency pyloric/gastric mill (fast/slow) activity via modulation of LPG intrinsic properties. Using current injections to manipulate neuronal activity, we found that gastric mill, but not pyloric, network neurons regulated the intrinsically generated LPG slow bursting. Conversely, selective elimination of LPG from both networks using photoinactivation revealed that LPG regulated gastric mill neuron firing frequencies but was not necessary for gastric mill rhythm generation or coordination. However, LPG alone was sufficient to produce a distinct pattern of network coordination. Thus, modulated intrinsic properties underlying dual-network participation may constrain which networks can regulate switching neuron activity. Further, recruitment via intrinsic properties may occur

in modulatory states where it is important for the switching neuron to actively contribute 53 to network output. 54 55 **Keywords** 56 Neuronal switching, central pattern generator, neuromodulation, coordination, 57 degeneracy 58 59 60 **New and Noteworthy** 61 We used small, well-characterized networks to investigate interactions between 62 rhythmic networks and neurons that switch their network participation. For a neuron 63 switching into dual-network activity, only the second network regulated its activity in that 64 network. Additionally, the switching neuron was sufficient but not necessary to 65 coordinate second network neurons, and regulated their activity levels. Thus, regulation 66 of switching neurons may be selective, and a switching neuron is not necessarily simply 67

a follower in additional networks.

68

69

Introduction

Oscillatory networks, including central pattern generator (CPG) networks generating rhythmic patterns such as walking, breathing, and chewing are highly modulated to promote adaptation (1–9). CPG flexibility includes neuronal switching, where neuronal participation changes from one network to another, or to multiple networks, via neuromodulation of intrinsic and/or synaptic properties (10–17). Although CPG neurons are typically involved in rhythm and/or pattern generation in their home network, it is unclear whether switching neurons from other networks also take on such an active role. For instance, they may be passive followers of a new pattern imposed upon them or become active contributors to rhythm and/or pattern generation in the new network.

The same or different neuron complements can be involved in rhythm generation, producing rhythmic activity and setting rhythm frequency, and pattern generation, determining the relative timing among network neurons (6, 18–21). In most examples with identified cellular-level mechanisms, switching neurons are recruited into another network via modulation of inter-network synapses (10, 12, 14), and passively follow this input, without contributing to network output, such as rhythm frequency or network neuron coordination. However, neurons may also be recruited into a second network via modulation of intrinsic properties (15, 17, 22, 23). Here we ask whether a switching neuron has an active role in a novel network when the recruitment mechanism is intrinsic to the switching neuron.

Due to their smaller numbers of identified, accessible rhythm and pattern generator neurons with characterized connectomes, plus identified modulatory inputs,

invertebrate systems are particularly useful for studying neuronal switching (24–32). In the crustacean stomatogastric nervous system (STNS), 26-30 neurons generate the pyloric (food filtering, ~ 1 Hz) and gastric mill (food chewing, ~ 0.1 Hz) rhythms (28, 29, 33–35). Furthermore, neuronal switching mechanisms are established in the STNS (10, 12, 17). Here, we examined whether a neuron recruited into dual-network activity via modulation of intrinsic properties contributes to rhythm and/or pattern generation in a second network.

In the crab, *Cancer borealis*, activation of the modulatory projection neuron 5 (MCN5), or bath application of the MCN5 neuropeptide Gly¹-SIFamide, increases pyloric frequency (26), activates the gastric mill rhythm (36), and switches the pyloric-only lateral posterior gastric (LPG) neuron (2 copies) into dual-frequency pyloric/gastric mill bursting (17). During the MCN5/Gly¹-SIFamide-elicited gastric mill rhythm, LPG is coordinated with the lateral gastric (LG), inferior cardiac (IC), and dorsal gastric (DG) network neurons (17, 36). While LPG slow bursting occurs via Gly¹-SIFamide modulation of LPG intrinsic properties (17, 23), how LPG is incorporated into the gastric mill network, and whether it contributes to rhythm and/or pattern generation is unknown. We hypothesized that LPG actively contributes to rhythm and pattern generation of the Gly¹-SIFamide gastric mill rhythm. Our results suggest that even if a switching neuron is not necessary for rhythm generation, it can contribute to pattern generation, shaping the activity strength and timing of other neurons in a second network.

Materials and Methods

<u>Animals</u>

Male *Cancer borealis* crabs were obtained from The Fresh Lobster Company (Gloucester, MA) and maintained in tanks containing artificial seawater at 10°C -12°C. For experiments, crabs were anesthetized on ice for 30-50 min before the foregut was removed from the animal during gross dissection, bisected, and pinned flat in a Sylgard 170-lined dish (Thermo Fisher Scientific). The STNS was dissected from the foregut during fine dissection and pinned in a Sylgard 184-lined petri dish (Thermo Fisher Scientific) (37). Throughout the dissection, the preparation was kept chilled in *C. borealis* physiological saline at 4°C.

Solutions

C. borealis physiological saline was composed of the following (in mM): 440 NaCl, 26 MgCl₂,13 CaCl₂,11 KCl,10 Trizma base, 5 Maleic acid, pH 7.4-7.6. Squid internal electrode solution contained the following (in mM): 10 MgCl₂, 400 Potassium D-gluconic acid, 10 HEPES, 15 NaSO₄, 20 NaCl, pH 7.45 (38). Gly¹-SIFamide (GYRKPPFNG-SIFamide, custom peptide synthesis: Genscript) (17, 36, 39–41) was dissolved in optima water (Thermo Fisher Scientific) at 10⁻² M and aliquots were stored at -20°C until needed. Gly¹-SIFamide aliquots were diluted in physiological saline at a final concentration of 5 μM. Picrotoxin (PTX) powder (Sigma Aldrich) was added directly to physiological saline at a final concentration of 10 μM and vigorously stirred for 45 min before use (PTX). Gly¹-SIFamide aliquots were added directly to PTX in physiological saline (10 μM) at a final concentration of 5 μM (SIF:PTX).

Electrophysiology

137

138

139

140

141

142

143

144

145

146

147

148

149

150

151

152

153

154

155

156

157

158

159

All preparations were continuously superfused with chilled C. borealis saline (8-10°C), or chilled saline containing Gly¹-SIFamide and/or PTX, as indicated. For uninterrupted superfusion of the preparation, all solution changes were performed using a switching manifold. Extracellular nerve activity was recorded using a model 1700 A-M Systems Amplifier and custom-made stainless-steel pin electrodes. Vaseline wells were built around nerves to isolate neuron signals, with one stainless-steel electrode wire placed inside the well, and the other outside the well as reference. Stomatogastric ganglion (STG) somata were exposed by removing the thin layer of tissue across the ganglion and observed with light transmitted through a dark-field condenser (MBL-12010 Nikon Instruments). Intracellular recordings were collected using sharp-tip glass microelectrodes (18-40 M Ω) tip-filled with squid internal electrode solution (see Solutions). STG neurons were identified based on their nerve projection patterns and their synaptic interactions with other STG neurons. MCN5 activation experiments included MCN5 stimulation via intracellular current injection, or extracellular inferior oesophageal nerve (ion) stimulation (30 Hz, tonic), in which a portion of the MCN1 axon was photoinactivaed (see below) as it entered the STG to prevent MCN1 neurotransmission during ion stimulation (17). MCN5 activation experiments were reanalyzed from 17. All intracellular recordings were collected using AxoClamp 900A amplifiers in current-clamp mode (Molecular Devices). All experiments were conducted in the isolated STNS following transection of the inferior and superior oesophageal nerves (ion and son, respectively, Fig. 1A). Electrophysiology recordings were collected

using data acquisition hardware (Micro1401; Cambridge Electronic Design), software (Spike2; ~5 kHz sampling rate, Cambridge Electronic Design), and laboratory computer (Dell).

Prior to all conducted experiments, unless otherwise indicated, the LP neuron was photoinactivated as described in 17. Briefly, the LP neuron was impaled with a sharp microelectrode (30-40 M Ω) that was tip-filled with AlexaFluor-568 hydrazide (10 mM in 200 mM KCl, Thermo Fisher Scientific) and back-filled with squid internal solution (see *Solutions*). The LP soma was filled using constant hyperpolarizing current injection (-5 nA) for 5-10 mins, and the current injection stopped to allow the dye to diffuse to the neurites and axon in the dorsal ventricular nerve (dvn) for 20-40 mins. The STG was then illuminated for 5-7 min using a Texas red filter set (560 ± 40 nm wavelength; Leica Microsystems). Complete photoinactivation was confirmed when the LP membrane potential reached 0 mV. This same protocol was used for simultaneous photoinactivation of both copies of the LPG neuron (LPG Killed).

LPG regulation via pyloric and gastric mill networks

To determine whether LPG gastric mill-timed (slow) bursting was regulated by the pyloric network in Gly¹-SIFamide, we compared LPG bursting activity before, during, and after 200 s duration hyperpolarizing current injections into both pyloric dilator (PD) neurons. Due to electrical coupling between the two PD neurons and the anterior burster (AB), the pacemaker neuron for the pyloric rhythm, hyperpolarization of the PD neurons sufficiently hyperpolarizes the AB neuron as well, and thus eliminates the pyloric rhythm (17, 42). To regulate the pyloric rhythm frequency, steady depolarizing (0

to +2.5 nA) or hyperpolarizing (-6 to -0.25 nA) current was injected into the two PD neurons. Each current level was maintained for the duration of five LPG slow burst cycles before changing pyloric frequency with a new holding current. In an additional set of experiments, pyloric frequency was regulated via steady current injection while LPG was isolated from gastric mill synaptic input via PTX application (17). Briefly, PTX (10) µM) in physiological saline was bath applied to the preparation for a minimum of 15 min to allow for PTX to sufficiently block inhibitory glutamatergic synapses (43, 44). PTX was judged effective when activity of the IC and ventricular dilator (VD) neurons in the medial ventricular nerve (mvn) overlapped with one another or, in cases where the pyloric neuron lateral pyloric (LP) neuron was intact, glutamatergic inhibitory postsynaptic potentials from LP in the PD neuron were eliminated, and LP and pyloric (PY) neuron activity overlapped in the lateral ventricular nerve (*lvn*) (17, 43, 44). Gly¹-SIFamide containing PTX (SIF:PTX, 5 µM:10 µM, respectively) was then applied to the preparation to examine the effects of pyloric frequency on LPG slow bursting with LPG isolated from glutamatergic synaptic inhibition.

183

184

185

186

187

188

189

190

191

192

193

194

195

196

197

198

199

200

201

202

203

204

205

To determine whether LPG slow burst activity was regulated by LG, IC, and/or DG gastric mill network neurons in Gly¹-SIFamide application, we reanalyzed a dataset from our previous study (17), in which LG, IC, and DG neurons were hyperpolarized (-2 to -4 nA, 200 s) individually and simultaneously for 200 s, followed by 200 s with no manipulation. LPG slow burst duration (time from the first to the last action potential within a burst) and cycle period (time between the first action potential of two consecutive bursts) were measured 200 s before, during, and after each LG, IC, and DG hyperpolarization. To test whether LPG slow bursting regulated LG, IC, and DG

gastric mill neuron activity, we measured LG, IC, and DG burst duration, cycle period, firing frequency ([number of spikes per burst – 1]/burst duration), and number of spikes per burst (the total count of action potentials between the first and last action potential of a burst) in Gly¹-SIFamide conditions with LPG intact versus LPG Killed.

Burst detection and identification

LPG neuron (2 copies) bursting activity was recorded in one or both of the lateral posterior gastric nerves (*lpgn*). LPG slow bursting was determined as described in 17. Briefly, a histogram containing LPG interspike intervals (ISIs) across an entire Gly¹-SIFamide application was generated using a custom-written MATLAB script (MathWorks) and the two largest peaks identified. The first peak (within ~0-0.5 s) included intra-burst intervals (interval between spikes during a burst), and the second peak (~0.5-2 s) included inter-burst intervals (interval between spikes between bursts). The mean ISI between these two peaks was calculated and used as a cutoff value to identify LPG bursting, such that an ISI above the cutoff indicated the end of one burst and the beginning of another. To select only LPG slow bursts from all LPG bursts identified with the ISI cutoff, we used a custom written Spike2 script that identifies LPG bursts with a duration greater than one pyloric cycle period (from PD burst onset to the next PD burst onset, ~1 s) (17).

To determine whether there was a relationship between pyloric frequency and LPG slow burst frequency, we measured LPG slow burst frequency (1/LPG slow burst cycle period) and burst duration in Gly¹-SIFamide-only and SIF:PTX conditions (5 LPG slow burst cycles, 30-200 s time window) across pyloric frequencies. To examine the

role of LPG slow bursting in LG, IC, and DG neuron regulation, we measured and compared LG, IC, and DG burst duration, cycle period, number of spikes per burst, and firing frequency across a 1200 s time window in Gly¹-SIFamide with LPG Intact and LPG Killed conditions.

LG, IC, and DG bursting activity was recorded either intracellularly or via extracellular nerve recordings (*Ign, mvn, dgn*, respectively). All bursts had at least 3 action potentials with a maximum of 2 s interspike interval. IC pyloric-timed bursts were determined by including only IC bursts with a minimum duration of 0.45 s (36), each separated by the duration of a PD (*pdn*) burst. IC gastric mill-timed bursts were determined by grouping together consecutive pyloric-timed IC bursts with a minimum burst duration of 0.45 s, including up to one IC burst < 0.45 s in duration if it occurred between other IC bursts that were at least 0.45 s.

Categorization of the gastric mill rhythm

To examine the role of LPG slow bursting in gastric mill network activity, we eliminated LPG actions by photoinactivating LPG (LPG Killed) with and without the influence of glutamatergic inhibitory synapses from network neurons LG, IC, and DG (PTX, 10 µM). To test whether LPG was necessary for generating the gastric mill rhythm, we used a combination of manipulations with 2-3 hr intervals between manipulations: Gly¹-SIFamide with LPG Intact (SIF:LPG Intact); Gly¹-SIFamide with LPG Killed (SIF:LPG Killed); Gly¹-SIFamide with Picrotoxin (SIF:PTX); and SIF:PTX with LPG Killed (SIF:PTX LPG Killed). Not all manipulations were performed in all preparations. Specific comparisons included SIF:LPG Intact (LPG Included in the

categorization analysis) versus SIF:LPG Intact (LPG Excluded from the categorization analysis) (n = 9, 41-142 cycles); SIF:LPG Intact (LPG Excluded) (n = 10, 41-142 cycles) versus SIF:LPG Killed (n = 10, 31-110 cycles); SIF:LPG Intact (LPG Included, n = 5, 29-105 cycles) versus SIF:PTX (LPG Included, n = 5, 52-114 cycles); and SIF:LPG Intact (LPG Excluded, n = 11, 29-105 cycles) versus SIF:PTX (LPG Excluded, n = 5, 52-114 cycles) versus SIF:PTX LPG Killed (n = 8, 8-124 cycles). For conditions without PTX application, the LP neuron was hyperpolarized to ensure LPG burst in gastric mill time (17). PTX was superfused prior to SIF:PTX, and PTX wash-out was confirmed by the presence of LP-elicited glutamatergic inhibitory post-synaptic potentials in an intracellular PD neuron recording (17, 43, 44).

The relative timing of neurons participating in the Gly¹-SIFamide rhythm is variable. Therefore, we applied a qualitative cycle-by-cycle analysis using LG as a reference to characterize gastric mill network coordination (Fig. 5, method adapted from (45)). First, LG, IC, DG, and LPG burst onsets and offsets were identified across a 1200 s time window in Spike2 and exported to MATLAB. IC, DG, and LPG burst onset and offset were compared relative to each LG cycle to determine the type of coordination for each neuron in each LG cycle. Then, the combination of coordination types was used to determine the network coordination among a total of four neurons (LG, IC, DG, and LPG) or three neurons (LG, IC, and DG), as indicated. For instance, complete coordination was defined as "All Coordinated" when all neurons assessed were associated with and defined as coordinated, with one cycle (Fig. 5). A neuron was considered to be "associated" with a current cycle if: burst onset and offset occurred within the current LG cycle; burst onset occurred near the end of the previous LG cycle

(less than 10% into the previous cycle) plus burst offset occurring in the current LG cycle; or burst onset occurred in the current LG cycle (at least 10%) and burst offset in the next LG cycle. For instance, in the example traces shown for "All Coordinated" the DG neuron was identified as coordinated because its burst onset was greater than 10% in that LG cycle (Fig. 5Bi). If a neuron was active across a complete LG cycle and extended beyond that LG cycle, the cycle was classified as "One Neuron Tonic" (Fig. 5). We did not have instances of more than one neuron being tonic. When one or more neurons were silent, that cycle was defined as "One Neuron Silent" or "All Silent", depending on the number not active in that cycle (Fig. 5). Finally, when IC, DG, and/or LPG neurons had more than one burst per LG cycle, or some other burst pattern that did not meet the above criteria, that cycle was defined as "One Neuron Uncoordinated" or "All Uncoordinated" (Fig. 5). Identified patterns from each preparation were accumulated and the mean percentage of cycles per category was calculated. To confirm that the results obtained were not due to multiple Gly¹-SIFamide applications or due to photoinactivation itself, we performed control experiments where (1) LPG was intact for two consecutive Gly¹-SIFamide applications and (2) two GM neurons were photoinactivated between two consecutive Gly¹-SIFamide applications. All analyses were conducted after Gly¹-SIFamide reached a steady state, approximately 10 mins after peptide wash-in.

294

295

296

297

293

275

276

277

278

279

280

281

282

283

284

285

286

287

288

289

290

291

292

Spike phase analysis

To quantify the relative timing relationships of gastric mill neurons, all LG neuron cycles were used as reference, regardless of coordination type. Each LG cycle was

divided into 100 bins and the number of spikes per bin quantified for all neurons, for all cycles, across the same 1200 s window used for categorical analysis. Action potentials and bursts were identified in Spike2 and exported to MATLAB. The number of spikes for each neuron, in each bin was accumulated using custom-written functions in MATLAB. Counts per bin were normalized to the total number of spikes in that neuron in each experiment, and expressed as a percent of total spikes.

Software and statistical analysis

Raw electrophysiology data were analyzed using functions and scripts that were written in Spike2 or MATLAB. Statistical analyses were performed using SigmaPlot (Systat). Graphs were plotted in SigmaPlot or MATLAB and imported into CorelDraw. All final figures were created using CorelDraw (Corel). Data were analyzed for normality using the Shapiro-Wilk Normality test before determining whether to use a parametric or nonparametric test on each dataset. Pearson correlation, One-way repeated measures (RM) ANOVA, Friedmann's one-way RM ANOVA on ranks, Paired t-test, Wilcoxon signed rank test, and *post hoc* tests for multiple comparisons were used as indicated. Overall p-values are reported in text, while *post-hoc* p-values are reported in Supplemental Tables, as indicated. Threshold for significance was p < 0.05. All data are presented as mean ± SEM.

Code accessibility

Scripts and functions used for analysis were written in Spike2 and/or MATLAB and are available at https://github.com/blitzdm/Fahoum_Blitz_2023_Coordination or upon request from D.M.B.

Supplemental Data

Supplemental Tables S1-S7:

https://figshare.com/articles/figure/FahoumBlitz_SupplementalTables_S1_S7/24886578

Results

The crab STNS is a region of the nervous system that controls the pyloric (food filtering, ~1 Hz) and gastric mill (food chewing, ~0.1 Hz) behaviors (Fig. 1) (28, 29). The STNS includes the paired commissural ganglia (CoG) and oesophageal ganglion (OG) containing modulatory projection neurons that have axonal projections to the STG (Fig. 1A). The STG is comprised of ~30 neurons that form CPG networks driving the pyloric and gastric mill rhythms (Fig. 1B). These networks and their modulatory inputs are well-characterized, including identified synapses between neurons (Fig. 1B) (4, 29, 46). The neuropeptide Gly¹-SIFamide is released from the modulatory commissural neuron 5 (MCN5), which projects through the *ion* and stomatogastric nerve (*stn*) to the STG (Fig. 1A). Bath application or neuronal release of Gly¹-SIFamide elicits an increase in pyloric frequency, activation of a gastric mill rhythm and switching of the pyloric-only LPG neuron (2 copies) into simultaneous dual pyloric/gastric mill timing (fast/slow timing, respectively) (Fig. 1C) (17, 26, 36). In saline conditions, LPG is pyloric-timed due to its

electrical coupling with the pyloric pacemaker group (AB/PD/LPG) (Fig. 1C, left) ((44, 47), S-RH Fahoum, DM Blitz, L Zhang, MP Nusbaum, unpublished). During Gly¹-SIFamide application, LPG maintains its fast pyloric-timed bursting activity via electrical coupling, and additionally generates slow bursting in time with the gastric mill rhythm (Fig. 1C, middle). When LPG is isolated from pyloric and gastric mill inputs via hyperpolarization of the two PD neurons and application of picrotoxin (PTX, 10 μM), respectively, LPG generates slow, gastric mill-timed bursting independently due to Gly¹-SIFamide modulation of LPG intrinsic properties (Fig. 1C, right) (17, 23). This mechanism of recruitment differs from other examples, in which modulation of synapses recruits a switching neuron into another network (10, 12, 13, 48).

During the MCN5/Gly¹-SIFamide gastric mill rhythm, the LPG neuron is coordinated with the LG, IC, and DG network neurons (17, 36). Although Gly¹-SIFamide modulation of LPG intrinsic properties is well-established as the mechanism for LPG to generate bursting at gastric mill rhythm frequency (17, 23), how LPG is incorporated into the gastric mill network, and whether it contributes to rhythm/pattern generation is not known. Here, we tested the hypothesis that LPG contributes to generating and shaping the Gly¹-SIFamide gastric mill rhythm. First, we examined whether pyloric and gastric mill activity regulated the intrinsically-generated LPG gastric mill-timed (slow) bursting in Gly¹-SIFamide. Then, we tested the role of LPG slow bursting in rhythm and/or pattern generation for the gastric mill network.

Pyloric network regulation of LPG

362

363

364

365

366

367

368

369

370

371

372

373

374

375

376

377

378

379

380

381

382

383

384

In Gly¹-SIFamide application, LPG periodically escapes its electrical coupling to the pyloric pacemaker group to burst in gastric mill time (17, 36). While this rhythmic electrical coupling input is not necessary for LPG to generate gastric mill-timed (slow) bursting, it is unknown whether the pyloric network regulates LPG slow bursting. In saline conditions, the AB neuron is the pacemaker for the pyloric rhythm, and its bursting activity controls rhythmic bursting in PD and LPG neurons through electrical coupling ((47, 49), S-RH Fahoum, DM Blitz, L Zhang, MP Nusbaum, unpublished). We tested whether the pyloric network regulates LPG slow bursting in Gly¹-SIFamide application by measuring LPG slow burst duration and cycle period pre-, during, and post- elimination of the pyloric rhythm via hyperpolarization of the two PD neurons. This manipulation sufficiently hyperpolarizes AB, and thus eliminates rhythmic pyloric-timed activity in the pacemaker group (PD, AB, LPG) due to electrical coupling between AB and PD neurons (42, 50). PD hyperpolarization also eliminates LPG pyloric-timed bursting due to electrical coupling, but not LPG gastric mill-timed (slow) bursting in Gly¹-SIFamide application (Fig. 2) (17). However, the previous study did not determine whether the LPG slow bursting in the absence of rhythmic pyloric input differed from control slow bursting. Shutting off the pyloric rhythm had no effect on LPG slow burst cycle period (Fig.

Shutting off the pyloric rhythm had no effect on LPG slow burst cycle period (Fig. 2Ai-Aii; PD ON-pre = 18.16 ± 1.66 , PD OFF = 14.69 ± 0.88 , PD ON-post = 15.36 ± 1.93 ; p = 0.231, n = 10, One-Way RM ANOVA) or slow burst duration (Fig. 2Aiii; PD ON-pre = 7.131 ± 1.66 , PD OFF 8.00 ± 0.48 , PD ON-post 7.22 ± 1.28 ; p = 0.273, n = 10, Friedman RM ANOVA on Ranks). One possible explanation for the inability of the

pyloric network to regulate LPG slow bursting could be that electrical coupling between LPG and PD neurons is rectifying, such that positive current flows more easily from PD to LPG, and negative current flows from LPG to PD (47). Thus, although PD hyperpolarization may not influence LPG slow bursting due to this rectification, the frequency of rhythmic AB/PD depolarizations might regulate LPG slow bursting.

385

386

387

388

389

390

391

392

393

394

395

396

397

398

399

400

401

402

403

404

405

406

407

To test for an influence of pyloric frequency on LPG slow bursting, we used steady current injections of hyperpolarizing or depolarizing current (-6 to +2.5 nA) into the two PD neurons to decrease or increase pyloric frequency. Across a range of pyloric frequencies, we found no correlation between pyloric frequency and LPG slow burst frequency (Fig. 2C) (r = 0.020, $r^2 = 0.0004$, p = 0.909, n = 4; Pearson correlation), or between pyloric frequency and LPG slow burst duration (r = 0.182, $r^2 = 0.033$, p =0.297, n = 4; Pearson correlation) (data not shown). To ensure that variable synaptic input from other gastric mill neurons (see Results below) was not masking the ability of the pyloric network to regulate LPG slow bursting, we also manipulated pyloric frequency with gastric mill network inputs blocked. Glutamatergic IC, LG, and DG synaptic actions were blocked with picrotoxin (PTX) and the pyloric frequency again regulated with depolarizing and hyperpolarizing current injections during Gly¹-SIFamide in the presence of PTX. There was some variability such as shorter LPG slow burst duration at a slower frequency in the example shown (Fig. 2Bi vs 2Bii) and a slower LPG slow burst frequency at a higher pyloric frequency (Fig. 2Biii). However, there was no correlation between pyloric frequency and LPG slow burst frequency (Fig. 2D; r = 0.098, $r^2 = 0.009$, p = 0.485, n = 8, Pearson Correlation), and no correlation between pyloric frequency and LPG slow burst duration (r = -0.140, $r^2 = 0.020$, p = 0.317, n = 8,

Pearson Correlation) (data not shown). Thus, the pyloric network was not able to regulate LPG slow bursting activity in Gly¹-SIFamide.

Regulation of LPG via gastric mill network neurons IC, DG, and LG

We previously found that, when gastric mill activity was eliminated, the overall percent of LPG slow bursting was not different from when gastric mill activity was present, thus the gastric mill network is not necessary for LPG to generate slow bursting (17). For instance, when gastric mill network neurons LG, IC, and DG are simultaneously hyperpolarized to eliminate their activity (LC/IC/DG OFF), LPG maintains its ability to generate slow bursting (Fig. 3A) (17). However, in the previous study we did not determine whether LPG slow bursting is regulated by the gastric mill network. Thus, we measured LPG slow burst duration and cycle period when LG, IC, and DG gastric mill neuron activity were eliminated via hyperpolarization, individually and collectively (Fig. 3, *re-analyzed dataset from 17*). Our measurements of LPG bursting activity were taken from *lpgn* recordings, in which both copies of LPG are present, making it difficult to assign action potentials to each individual LPG. Thus, we did not quantify LPG number of spikes per burst or firing frequency.

Hyperpolarizing gastric mill neurons did influence LPG slow bursting. Specifically, hyperpolarization of IC elicited a decrease in LPG slow burst cycle period but did not affect LPG slow burst duration (Fig. 3Bi, Bii, LPG cycle period: p = 0.029, Supplemental Table S1; LPG burst duration: p = 1.000, Supplemental Table S1; n = 10, One-way RM ANOVA). When LG was hyperpolarized, both LPG slow burst cycle period and burst duration were decreased (Fig. 3Bi, Bii, LPG cycle period: p < 0.001, Supplemental

Table S1; LPG burst duration: p = 0.003, Supplemental Table S1; n = 12, One-way RM ANOVA). DG hyperpolarization elicited an increase in LPG slow burst cycle period but did not affect LPG slow burst duration (Fig. 3Bi, Bii, LPG cycle period: p = 0.008, Supplemental Table S1; LPG burst duration: p = 0.370, Supplemental Table S1; n = 8, One-way RM ANOVA). During simultaneous hyperpolarization of LG, IC, and DG neurons (LG/IC/DG OFF), LPG cycle period was shorter, however, LPG slow burst duration was not affected (Fig. 3Bi, Bii, LPG cycle period: p = 0.017, Supplemental Table S1; LPG burst duration: p = 0.824, Supplemental Table S1; n = 6, One-way RM ANOVA). Thus, although LPG slow bursting can occur without gastric mill inputs, this slow bursting is regulated by gastric mill network neurons.

LPG contributions to gastric mill rhythm and pattern generation

Thus far, we found that gastric mill network neurons LG, IC, and DG regulate LPG slow burst activity. However, the role of a switching neuron in a second network when recruited via modulation of intrinsic properties is unknown. Thus, we examined the role of LPG switching into the gastric mill network during Gly¹-SIFamide application.

One way to test this would be to hyperpolarize LPG neurons to eliminate their activity and compare LG, IC, and DG burst parameter measurements between LPG active versus LPG inactive. However, due to rectifying electrical coupling between LPG and PD neurons (47), negative current injections into LPG would hyperpolarize AB/PD and slow or eliminate the pyloric rhythm and thus not test the impact of only altering LPG activity. Instead, we used photoinactivation (see Methods; 44) to selectively eliminate LPG activity without eliminating the pyloric rhythm and compared LG, IC, and DG

gastric mill neuron activity in LPG intact versus LPG photoinactivated (LPG Killed) conditions (Fig. 4).

Since Gly¹-SIFamide modulates LPG to become an intrinsic burster in the gastric mill network during Gly¹-SIFamide application (5 μM) (17, 23), we first determined whether LPG slow bursting is necessary for generating the Gly¹-SIFamide-elicited gastric mill rhythm (Fig. 4). When LPG was intact and dual-active (pyloric and gastric mill-timed, *lpgn*), the gastric mill neurons LG (*lgn*), IC (*mvn*), and DG (*dgn*) generated gastric mill-timed bursting activity (Fig. 4Ai). Following photoinactivation of LPG (2 copies, LPG Killed), the LG, IC, and DG neurons maintained their bursting activity, in all preparations tested (Fig. 4Aii, n = 10/10). Thus, LPG slow bursting is not necessary for gastric mill rhythm generation.

Quantifying LG, IC, and DG activity parameters, we found that LG and DG firing frequency was decreased after LPG Killed (Fig. 4B, LG: p = 0.0008, Supplemental Table S2, n = 12, paired t-test; DG: p = 0.002, Supplemental Table S2, n = 10, Wilcoxon Signed Rank Test). LPG did not regulate IC firing frequency (Fig. 4B, IC: p = 0.472, Supplemental Table S2, n = 11, paired t-test), or cycle period, burst duration, or number of spikes per burst for LG, IC, and DG (Fig. 4B; Cycle Period: LG, p = 0.371, n = 12, paired t-test; IC, p = 0.173, n = 11, paired t-test; DG, p = 0.102, n = 11, Wilcoxon Signed Rank Test; Burst Duration: LG, p = 0.928, n = 12, paired t-test; IC, p = 0.438, n = 11, paired t-test; DG, p = 0.123, p = 11, Wilcoxon Signed Rank Test; Number of Spikes per Burst: LG, p = 0.082, n = 12, paired t-test; IC, p = 0.505, n = 11, paired t-test; DG, p = 0.230, p = 10, paired t-test; Supplemental Table S2).

During Gly¹-SIFamide application, IC gastric-mill timed bursts (Fig. 4A, blue boxes; see Methods for criteria) sometimes consist of multiple bursts that are interrupted in pyloric time (Fig. 4A, red arrows) (17, 36). Thus, in addition to examining LPG effects on IC gastric mill timing, we examined whether IC pyloric-timed activity was regulated by LPG slow bursting and found that pyloric-timed IC bursting was not different after LPG photoinactivation (Fig. 4B, Pyloric-IC; p=0.206 – 0.900, Supplemental Table S2). Overall, these results indicate that while LPG is not necessary for generating the gastric mill rhythm, it does play a role in regulating some aspects of gastric mill network neuron activity.

LPG is not necessary for coordinating the Gly¹-SIFamide gastric mill rhythm

CPG pattern generation involves the relative timing, i.e., coordination of network neuron activity (2, 6, 51–54). Additionally, the strength of neuron activity, including firing frequency, is important for muscle and other targets outside the network, but can also be important for interactions between synaptically connected network neurons, and thus impact coordination (24, 55–58). Since LPG influences gastric mill neuron firing frequency, we next examined whether LPG was necessary for coordinating LG, IC, and DG neurons in Gly¹-SIFamide.

Typically, in Gly¹-SIFamide (5 μM), the pattern of the gastric mill rhythm is variable both within and across preparations, posing a challenge to detect changes in network coordination between the intact and LPG killed conditions. Thus, we used a qualitative approach in which we categorized coordination among gastric mill network neurons on a cycle-by-cycle basis, using the LG neuron as the reference neuron (Fig. 5,

see Methods, adapted from (45)). Briefly, LG, IC, DG, and LPG burst starts and stops were identified across a 1200 s time window, and coordination among three (LG, IC, and DG) or four (LG, IC, DG, and LPG) neurons was determined based on a series of coordination types observed in Gly¹-SIFamide-elicited gastric mill rhythms. We considered "coordination" to be instances with 1:1 relationships between neuron bursts. For instance, "All Coordinated" indicates a single burst in other network neurons occurring within one LG cycle (Fig. 5A, "All Coordinated"). In addition, "All Coordinated" includes burst onset occurring near the end of the previous LG cycle (less than 10% into the previous cycle) plus burst offset occurring in the current LG cycle; or burst onset occurring in the current LG cycle (at least 10%) and burst offset in the next LG cycle. For instance, in figure 5Bi, the first "All Coordinated" cycle has IC and LPG bursts with onsets and offsets within the LG cycle. In addition, the DG neuron onset in this cycle was greater than 10% and had an offset in the next cycle (Fig. 5Bi, "All Coordinated"). If a neuron was active across a complete LG cycle and extended beyond that LG cycle, the cycle was classified as "One Neuron Tonic" (Fig. 5, "One Neuron Tonic"). DG was the only neuron that exhibited "Tonic" activity. When one or more neurons were silent, that cycle was defined as "One Neuron Silent" or "All Silent", depending on the number not active in that cycle (Fig. 5, "One Neuron Silent", "All Silent"). Finally, when IC, DG, and/or LPG neurons had more than one burst per LG cycle, or some other burst pattern that did not meet the above criteria, that cycle was defined as "One Neuron Uncoordinated" or "All Uncoordinated" (Fig. 5). Within each preparation, we found that a single coordination type might only persist for a single cycle at a time. For instance, in the example traces in figure 5Bi, one preparation exhibited cycles categorized as "One

499

500

501

502

503

504

505

506

507

508

509

510

511

512

513

514

515

516

517

518

519

520

521

Neuron Tonic", plus an alternation between "All Coordinated" and "One Neuron Silent" cycles (Fig. 5Bi). Three additional preparations provide examples of additional types of coordination that were observed across preparations (Fig. 5Bii). Given the level of variability of the gastric mill rhythm even within each preparation, we quantified the percentages of coordination types across preparations and conditions on a per cycle basis.

522

523

524

525

526

527

528

529

530

531

532

533

534

535

536

537

538

539

540

541

542

543

544

First, we conducted a set of control experiments to verify that repeated Gly¹-SIFamide applications have the same effects, and that photoinactivation of two neurons does not alter the gastric mill network response to Gly¹-SIFamide. In these control experiments we categorized gastric mill rhythm coordination in conditions where (1) two consecutive Gly¹-SIFamide applications occurred with no neurons photoinactivated and (2) two gastric mill (GM) neurons were photoinactivated before a second Gly¹-SIFamide application. GM neurons are not excited by Gly¹-SIFamide (36) and provide an assay for any generalized effects of photoinactivation on the STG. To assess any effects on coordination, identified gastric mill rhythm coordination patterns from each preparation were accumulated and the mean percent of cycles per category was calculated and represented in a stacked bar graph, where each colored bar represents one category, and each collection of bars indicates one experimental condition analyzed (Fig. 6). Consecutive Gly¹-SIFamide applications (Fig. 6, SIF App 1 vs. SIF App 2) and photoinactivation of two GM neurons (Fig. 6, GM Intact vs. GM Killed) did not affect gastric mill rhythm coordination. Specifically, there were no signficiant differences in the percent of cycles in each category between SIF App 1 and SIF App 2 (p = 0.77 - 1; Supplemental Table S3) or between GM Intact and GM Killed (p = 0.206 - 1.0;

Supplemental Table S4). These results gave us confidence that we could use multiple applications of Gly¹-SIFamide before versus after photoinactivating both copies of the LPG neurons and assess whether there were effects on coordination due to the selective elimination of LPG.

In the "SIF:LPG Intact (LPG Included)" condition, IC, LPG, and DG neuron activity was examined relative to LG activity to determine network coordination. In this control condition, $20.71 \pm 3.77\%$ of cycles were "All Coordinated", $19.56 \pm 6.42\%$ were "One Neuron Uncoordinated", $14.91 \pm 6.01\%$ were "One Neuron Tonic", $19.01 \pm 4.34\%$ cycles were "One Neuron Silent", $25.24 \pm 5.08\%$ cycles were "All Uncoordinated", 0% were "All Tonic", and $0.48 \pm 0.26\%$ were "All Silent" (Fig. 7A, Bi). This plot highlights the variable nature of the Gly¹-SIFamide gastric mill rhythm.

There are some differences between bath applied and neuronally released Gly¹-SIFamide (36),and thus we were interested in whether the gastric mill rhythm elicited by MCN5-released peptide was also variable in its coordination. The previous study indicated that DG was more coordinated in response to MCN5 stimulation, but this was measured as the number of preparations with coordinated DG activity and did not consider coordination on a per cycle basis . Here, we tested the cycle-by-cycle coordination of all gastric mill neurons, including LPG, by tonically stimulating the modulatory projection neuron MCN5 (30 Hz stimulation, 200 s time window), and found that there were $24.87 \pm 14.71\%$ "All Coordinated" cycles, $4.0 \pm 4.0\%$ "One Neuron Uncoordinated" cycles, $3.08 \pm 3.08\%$ "One Neuron Tonic" cycles, $21.73 \pm 11.20\%$ "One Neuron Silent" cycles, $42.99 \pm 9.16\%$ "One Neuron Uncoordinated" cycles, 0% "All Tonic" cycles, and $3.33 \pm 3.33\%$ "All Silent" cycles (n=5; data not shown). We did not

perform a statistical analysis on bath-applied versus MCN5-released Gly¹-SIFamide due to differences in analysis time windows (1200 s vs. 200 s). However, it appears qualitatively that the extent of gastric mill neuron coordination is similar in bath-applied Gly¹-SIFamide compared to neuronal release from MCN5.

568

569

570

571

572

573

574

575

576

577

578

579

580

581

582

583

584

585

586

587

588

589

When LPG was excluded [SIF:LPG Intact (LPG Excluded)] from the categorization analysis in the SIF:LPG Intact condition, the percentage of cycles for "All Coordinated" and "One Neuron Silent" was higher and "All Uncoordinated" was lower, while there was no difference for each of the other categories (Fig. 7Bi, Supplemental Table S5, All Coordinated: p = 0.008, paired t-test; One Neuron Silent: p = 0.0496, paired t-test; All Uncoordinated: p < 0.001, Wilcoxon signed rank test; n = 9). These differences in mean percentage of cycles per category are likely due to a fourth component (LPG) included in pattern identification in the SIF:LPG Intact (LPG Included) measurements. For instance, in two consecutive cycles in figure 5Bii (leftmost traces), the IC and DG neurons are "All Coordinated" with LG, however, with the addition of LPG, the overall coordination indicates that the two cycles are "One Neuron Uncoordinated". While the inclusion of LPG in the categorization analysis provides more information about the nature of coordination among the gastric mill neurons and LPG slow bursting, it does not address our question of whether LPG plays an important role in mediating coordination among LG, IC, and DG neurons. Thus, to address this question, we chose to identify types of network coordination by including only LG, IC and DG neurons to maintain consistency between SIF:LPG Intact and SIF:LPG Killed conditions.

When LPG was photoinactivated, we found that the mean percentage of LG cycles that were "All Coordinated" was unchanged between SIF:LPG Intact (LPG excluded) and SIF:LPG photoinactivated (Killed) conditions (Fig. 7A, Bii; Supplemental Table S5, SIF:LPG Intact: 34.78 ± 4.63%, SIF:LPG Killed: 31.01 ± 4.92%; p = 0.597, n = 10, paired t-test). This suggests that LPG slow bursting is not necessary for coordinating the gastric mill rhythm in Gly¹-SIFamide. Furthermore, although gastric mill rhythm coordination patterns were variable from cycle-to-cycle (Fig. 5Bi), we observed that the variability in coordination types was similar between SIF:LPG Intact and SIF:LPG Killed conditions (Fig. 7Bii, Coeffficient of variation [CV] for SIF:LPG Intact vs SIF:LPG Killed: All Coordinated, 0.42 vs 0.50; All Uncoordinated, 1.15 vs 1.08; One Uncoordinated, 1.72 vs 2.19; One Tonic, 0.94 vs 1.64; One Silent, 0.53 vs 0.56; All tonic, 3.16 vs N/A; All Silent, 1.72 vs 1.69). Thus, the variability of gastric mill coordination was not due to LPG slow bursting.

While our category approach indicated that there was no difference in the percentage of 1:1:1 bursting activity of LG, IC, and DG neurons with or without LPG, it did not allow us to address the specific pattern and whether there was a change in the relative timing, i.e., phase relationships of the neurons. We wanted to describe the specific relative timing of neuronal activity, for instance, to determine whether DG and LG are coincident or out of phase with each other, regardless of whether there is 1:1 coordination of all neurons in each cycle. To do this, we quantified spiking activity of all neurons, across all cycles, regardless of the type of coordination, again setting LG as the reference neuron. This allowed us to visualize all neuronal activity without limiting the analysis to ~30% of the cycles that were fully coordinated. To determine whether

LPG was involved in mediating the relative timing among LG, IC, and DG network neurons we compared the pattern of spiking with SIF:LPG intact versus SIF:LPG killed (Fig. 7C). Each cycle began with the onset of an LG burst and ended at the start of the subsequent LG burst and was divided into 100 bins. In the control condition, LG spiking extended for ~40% of the cycle which largely overlapped with spiking in the IC neuron (Fig. 7Ci). DG spiking occurred throughout the cycle with a tendency to have fewer spikes per bin mid-cycle across preparations (colored lines) and also evident in the average activity (thick black line, n = 10), which overlapped with the highest degree of spiking in LPG (LPG slow bursts). In the SIF:LPG Killed condition (Fig. 7Cii), the pattern of activity appeared similar, with LG and IC coactive for the first ~40% of the cycle, and DG activity was spread across the phase, although it appeared biased toward the end of the cycle. A few preparations which had more DG activity early in the phase in the control condition, did not have such high activity after LPG was killed, but overall there was not a dramatic shift in the pattern, indicating that LPG was not necessary for coordinating the other gastric mill neurons.

628

629

630

631

632

633

634

635

613

614

615

616

617

618

619

620

621

622

623

624

625

626

627

LPG is capable of coordinating gastric mill network neurons

Thus far, we examined the role of LPG in mediating coordination among gastric mill neurons by removing LPG synaptic effects via photoinactivation. Although LPG was not necessary for gastric mill coordination (Fig. 7), we did find that LPG regulated LG and DG firing frequency (Fig. 4), suggesting some role for LPG in determining gastric mill network activity in Gly¹-SIFamide. In CPG networks, there can be degeneracy at the cellular and synaptic levels, which may only become evident during a perturbation (59,

60). It was possible that there is synaptic degeneracy among gastric mill neurons in Gly¹-SIFamide, such that eliminating LPG via photoinactivation does not disrupt coordination due to the other synapses present among LG, IC, and DG neurons. Thus, LPG photoinactivation alone may not enable us to conclude whether LPG can play an active role in the gastric mill network. In the crab STG, the LPG neuron is cholinergic, while LG, IC, and DG neurons are glutamatergic. This distinction in neurotransmitters enabled us to test whether cholinergic LPG synapses can coordinate gastric mill neurons (Fig. 8A).

636

637

638

639

640

641

642

643

644

645

646

647

648

649

650

651

652

653

654

655

656

657

658

We found that LPG could coordinate gastric mill neurons on its own, but in a different pattern. For instance, in an example cycle in the control Gly¹-SIFamide condition (SIF:LPG Intact, Fig. 8A, left, blue outline), LG and IC are coactive, LPG is active near the middle of the cycle (blue box) and DG activity begins after LPG. However, when inhibitory glutamatergic synapses were blocked with picrotoxin (PTX, 10 μM) during Gly¹-SIFamide application (SIF:PTX:LPG Intact), LG, IC, and DG neuron bursting overlapped at the beginning of cycle (e.g., blue outline) and alternated with LPG bursting (Fig. 8A middle, blue box, n = 4/5). Across five experiments in which we applied Gly¹-SIFamide, followed by Gly¹-SIFamide + PTX (SIF:PTX:LPG Intact), we applied our categorical analysis to all four neurons (LG, IC, LPG, and DG) and found that the mean percentage of "All Coordinated" activity was not different in SIF:PTX LPG Intact compared to SIF:LPG Intact (Fig. 8Bi, Supplemental Table S6, p = 0.148, n = 5, paired t-test), Furthermore, there were no differences between SIF:PTX LPG Intact and SIF:LPG Intact for any of the other categories (Supplemental Table S6). However, although the number of coordinated cycles was not different, there was a qualitative

change in the pattern of neuronal activity (Fig. 8A). To quantify this, we again analyzed neuronal spiking (100 bins) across each cycle using LG as the reference neuron. In SIF:PTX:LPG Intact, there was a shift compared to SIF:LPG Intact, with DG now largely coactive with LG and IC, and LPG primarily active at the end of the cycle (Fig. 8C, right). Overall, the pattern shifted from triphasic (IC/LG, LPG, DG) to biphasic (LG/IC/DG, LPG), and indicated that LPG can be sufficient to coordinate gastric mill neurons, even though it is not necessary for the baseline pattern generation.

Given the prevalence of electrical coupling in the STG as in other networks (49), it remained possible that in the absence of glutamatergic inhibition among the LG, IC, and DG neurons, electrical coupling coordinated their activity. To determine whether it was electrical coupling, or the LPG cholinergic inhibition that was responsible for the coordination in SIF:PTX:LPG Intact, we combined SIF:PTX application with LPG neuron photoinactivation. In this condition, LG, IC, and DG synapses are blocked via PTX, and LPG activity was selectively eliminated, thus eliminating all intra-network chemical synapses among these gastric mill neurons (35). In this condition, although there was some bursting, particularly in the DG neuron (Fig. 8A, right, dgn; n = 6/8), there was no obvious coordination (Fig. 8A, right, SIF:PTX LPG Killed).

To compare the LPG Killed condition with other conditions, we did not include LPG in the categorical analysis and used a larger data set of three conditions (SIF:LPG Intact, n=10; SIF:PTX:LPG Intact. n=5; SIF:PTX:LPG Killed, n=8). We found that the "All Coordinated" category decreased, while "All Uncoordinated" increased (Fig. 8Bii, Supplemental Table S7; SIF:LPG Intact [n = 10] vs. SIF:PTX LPG Intact [n = 5] vs. SIF:PTX:LPG Killed [n = 8], All Coordinated: p = 0.004, One-way ANOVA; All

Uncoordinated: p = 0.04, Kruskal-Wallis one-way ANOVA on ranks). All other categories were unchanged across conditions (Fig. 8Bii; Supplemental Table S7). Therefore, the overlapping activity observed between LG, IC, and DG in SIF:PTX was not due to electrical coupling among these neurons, but due to chemical synaptic input from LPG, which is functional in the Gly¹-SIFamide modulatory state (61). The remaining small percentage of "All Coordinated" cycles in the SIF:PTX:LPG Killed condition suggested a lack of timing relationship among the neurons. This was further evident when examining spiking activity across all cycles in the SIF:PTX:LPG Killed conditions (Fig. 8D, right). Although some bursting activity was evident in some preparations (Fig. 8A, right; Fig. 8D, right, jagged individual experiment lines, IC and DG), overall the activity of the three remaining gastric mill neurons was relatively uniformly distributed across LG "cycles". Note, we used standard interspike intervals to objectively identify LG bursts (see Methods). For some experiments in the SIF:PTX:LPG Killed condition, this resulted in very few LG bursts due to almost tonic LG activity (number of LG bursts: 8 to 124). Thus, although not necessary for rhythm generation or network coordination, LPG gastric mill-timed bursting is sufficient to coordinate gastric mill network neurons in the Gly¹-SIFamide modulatory state in the absence of other intra-network chemical synapses.

700

701

702

703

704

682

683

684

685

686

687

688

689

690

691

692

693

694

695

696

697

698

699

Discussion

To understand the implications of neuronal switching, it is important to determine the bidirectional interactions between switching neurons and each of their networks. In the present study, we found that the slow gastric mill (~0.1 Hz), but not the faster pyloric

(~1 Hz), network regulated LPG slow bursting. Additionally, we tested whether LPG regulates the output of its second network, when in its dual-network state. We found that LPG is not necessary for gastric mill rhythm generation, but does regulate aspects of network neuron activity and has the ability to coordinate the entire network. These findings provide novel insight into the roles of a switching neuron which generates dual-network activity via a combination of electrical synapse (pyloric) and intrinsic (gastric mill) mechanisms.

Switching neuron intrinsically-generated activity is not regulated by its "home" network

The inability of physiological changes in the pyloric network to regulate LPG gastric mill-timed bursting is surprising because LPG gastric mill-timed bursting is intrinsically generated and voltage-sensitive (17). Although the electrical coupling between LPG and the AB/PD pacemaker group is rectifying, it is an incomplete rectification. Specifically, positive current flows preferentially, but not exclusively, from PD to LPG, and similarly for negative current from LPG to PD (47). Thus, we expected that a depolarizing or hyperpolarizing shift in the voltage of the PD neurons, sufficient to alter the voltage-dependent intrinsic oscillations of the pyloric pacemaker, would affect LPG slow bursting, at the very least when PD neurons were depolarized. One possible explanation for a lack of regulation from AB/PD fast bursting to LPG slow bursting is a decrease in electrical coupling strength between these neurons in the Gly¹-SIFamide modulatory state. However, this possibility is unlikely, as LPG can regulate AB/PD activity during its slow bursts ([(36)], B Gnanabharathi, S-RH Fahoum, DM Blitz, unpublished observations). An alternative possibility for the lack of pyloric regulation of

LPG slow bursting is the time-dependence of the intrinsic currents underlying LPG slow bursting. For instance, in a gastric mill rhythm elicited by the modulatory projection neuron MCN1, rhythmic release of its neuropeptide, CabTRP-la causes rhythmic waxing and waning of a modulator-activated inward current (IMI) necessary for gastric mill neuron bursting. A similar gastric mill rhythm version is produced by bathapplication of the neuropeptide CabPK, but in this case a time- (and calcium-) dependent current is also necessary for gastric mill neuron rhythmic activity (33, 42, 62, 63). However, in both gastric mill rhythms, the pyloric rhythm does regulate the gastric mill rhythm. A difference between the rhythmic oscillations in gastric mill neurons in the preceding examples and the LPG slow bursting, is that the LPG slow bursts are intrinsically generated and do not require input from other gastric mill neurons (17). In the MCN1- and CabPK-elicited rhythms, in addition to the mentioned intrinsic currents, reciprocal inhibition between LG and Int1 is necessary for their rhythmic activity (33, 64). Our findings suggest that the intrinsic currents underlying the LPG slow bursting (23) may overwhelm the current through the electrical synapses, even in the preferential direction of depolarizing current flow from PD to LPG. However, the lack of control by the pyloric network may be due to more than just the amplitude of the currents, as the interactions between electrical coupling and intrinsic currents can be complex and generate unexpected cellular and circuit level effects (49, 65–67).

747

748

749

750

728

729

730

731

732

733

734

735

736

737

738

739

740

741

742

743

744

745

746

Switching neuron intrinsically generated activity is regulated by its second network

Unlike turning off the pyloric rhythm, eliminating the activity of individual, or all three gastric mill network neurons (LG, DG, IC) altered LPG neuron gastric mill-timed

(slow) bursting. These gastric mill neurons altered LPG burst cycle period and/or burst duration despite LPG slow bursting being generated via intrinsic currents (17, 23). In baseline conditions IC, LG, and DG do not have functional synapses onto LPG. Thus, Gly¹-SIFamide modulation of intra-network synapses between LPG and the other gastric mill neurons is an additional important modulatory action of Gly¹-SIFamide (61). Intrinsic bursting that is further shaped by synaptic input from the network is a common motif in CPG and other rhythmic neural networks (68–71). For example, the pyloric pacemaker ensemble does not require any synaptic input to generate the rhythm, but cycle period variability is decreased by rhythmic feedback from the LP neuron (58, 72). Thus, regulation of endogenous switching neuron bursting by the second network can be important for additionally shaping switching neuron activity to produce appropriate behavior.

The role of a switching neuron in rhythm and pattern generation in a second network

Initially, it was thought that switching neurons recruited into a second network simply act as follower neurons to carry out patterns of activity determined by the synapses that recruit them (10, 12, 14). However, the role of a switching neuron recruited into a second network via modulation of intrinsic properties had not been examined. One possible role for switching neuron activity in a second network is rhythm generation, to drive CPG rhythmicity and set its frequency (6, 73–77). Because LPG generates endogenous gastric mill-timed bursting during Gly¹-SIFamide application (17), it was possible that LPG was integral for rhythm generation. However, we found that eliminating LPG activity did not eliminate pyloric or gastric mill rhythmic activity,

demonstrating that LPG activity, including its intrinsically generated slow bursting, is not necessary for rhythm generation in either network.

Another possible role for a switching neuron is pattern generation, where neurons determine the activity levels and relative timing among network neurons (74, 78, 79). Here, we found that LPG regulates LG and DG firing frequency. These neurons are members of the gastric mill CPG and motor neurons controlling the movements of the lateral teeth and medial tooth, respectively. The LG and DG firing frequency is thus relevant for the efficacy of synaptic transmission centrally within the CPG, and at the neuromuscular junction (80–82). As a consequence, the impact of LPG on DG and LG activity level can alter behavior directly via changes in muscle contractions, and potentially indirectly through changes in CPG targets of LG and DG.

We found that LPG was not necessary to maintain coordination among gastric mill neurons and there was little difference in the timing relationships in the absence of LPG. Given the variability of the Gly¹-SIFamide gastric mill rhythm, our analysis might not have been sensitive enough to detect changes in coordination in the absence of LPG, or there might be degeneracy such that other synapses contribute the same function as the LPG neurons (83, 84). However, when other chemical synapses among gastric mill neurons were blocked with picrotoxin, LPG fully coordinated the activity of the other gastric mill network neurons, but with different timing relationships. The DG neuron was both the most variable, and the most different when LPG was the sole contributor to network coordination. The variability in DG activity may reflect the absence of sensory feedback, such as muscle proprioceptor feedback (85–88), although DG is more regular during other in vitro gastric mill rhythms (33, 89, 90). Unlike

DG, the LG and IC neurons were consistently out of phase with LPG across conditions. The prolonged IC bursting occurring in the Gly¹-SIFamide gastric mill rhythm is a hallmark of this rhythm, which does not occur in multiple other gastric mill rhythm versions (25, 64, 89). The ability of LPG to regulate the timing of IC as well as LG emphasizes the important role that LPG is capable of playing, despite it being a temporary visitor from the pyloric network. This capability appears to be mediated by Gly¹-SIFamide modulation of typically ineffective synapses (61). Conversely, in the lobster STNS, peptide-mediated enhanced synaptic input from the cardiac sac network drives gastric mill neurons in a conjoint pattern without any feedback contributions from the recruited neurons (48). It is possible that the particular intrinsic properties and subsequent strong firing in LPG (23) are necessary for LPG to regulate the activity of other gastric mill neurons. In other instances in which modulation of intrinsic properties contributes to neuronal switching, it removes a neuron from participation in a network. This includes metabotropic acetylcholine actions that eliminate the sigh component of dual-eupneic/sigh activity in mouse respiratory neurons and modulatory suppression of plateau properties that removes the VD neuron from the lobster pyloric circuit, with its absence important for the activity of another neuron (10, 15). It seems likely that different modulators could alter intrinsic properties to instead recruit these neurons, similar to LPG, which may enable them to then make contributions to a second network, but in these and other systems involving switches between single and dual-network activity, those details are not yet available (10, 15, 91, 92). Here we find that modulatorelicited intrinsic LPG slow bursting enables LPG to generate activity at the gastric mill

797

798

799

800

801

802

803

804

805

806

807

808

809

810

811

812

813

814

815

816

817

818

rhythm frequency, plus contribute to patterning the network output and thereby determine the version of behavior produced.

821

822

823

824

825

826

827

828

829

830

831

832

833

834

835

836

837

838

839

840

841

819

820

Synaptic degeneracy as a mechanism for variability in pattern generation

Degeneracy and variability are important themes in motor systems, as they promote network stability and flexibility, respectively (59, 60, 93). Degeneracy also includes neuromodulatory actions, in which distinct modulators converge on the same ionic current to stabilize neuron bursting activity (5, 94–96). Furthermore, degeneracy of ion channels or synapses contributes to different mechanisms for the same motor pattern under different modulatory states (63, 64, 84). In the Gly¹-SIFamide modulatory state, partial synaptic degeneracy among LG, IC, LPG, and DG neurons may be important for enabling the gastric mill network to carry out multiple coordination patterns. Variability in phase relationships can be periodic, such as the regular switches between peristaltic and near synchronous heart tube contractions in the medicinal leech neurogenic heartbeat system (97). It is unknown whether similar periodic switches in phase relationships occur with the Gly¹-SIFamide rhythm in vivo, but there are examples of other versions of the gastric mill motor pattern switching on a per cycle basis. For instance, endoscopic recordings in the intact spiny lobster *Panulirus* interruptus foregut reveal cycle by cycle switches in the spontaneous chewing motor pattern, in vivo EMG recordings in the lobster *Homarus gammarus* demonstrate switches in phasing related to feeding, and physiologically-timed activation of a sensory neuron can cause a transient switch in the gastric mill pattern in the isolated *C. borealis* STNS (98–100). In lobster, LPG is a gastric mill network neuron. However, it is

interesting that one of the switches in phasing observed in the lobster in vivo studies was a change in the LPG gastric mill phase relationship (98). Much less is known about LPG activity in the gastric mill rhythm in crabs, in which it is primarily active with the pyloric rhythm but does have the ability to switch into the dual-network activity as discussed in this study. In vitro the triphasic Gly¹-SIFamide pattern occurs. However, we do not know if there are distinct behavioral states, or sensory stimuli that might bias the Gly¹-SIFamide modulated network toward the biphasic pattern observed in SIF:PTX, or whether switching between both patterns of coordination might occur within the same condition.

Conclusion

Here, we found that although LPG is not necessary for gastric mill rhythm generation in the Gly¹-SIFamide modulatory state, it contributes to pattern generation. Specifically, LPG regulates the activity level of other gastric mill neurons in our typical in vitro conditions. Additionally, we found that in the absence of glutamatergic chemical transmission, LPG slow bursts are sufficient to coordinate the remainder of the gastric mill neurons. This suggests degeneracy in synaptic connectivity and the possibility that there is a distinct behavioral or modulatory state in which LPG plays a dominant role in coordinating gastric mill neurons. Overall, we found that a switching neuron that is recruited to oscillate at a second network frequency can play an active role in the second network. This contrasts with a passive role for switching neurons recruited via internetwork synapses. It will be interesting to examine other instances of intrinsic property modulation as a mechanism of recruiting a neuron into another network to

determine if this dichotomy between modulation of intrinsic and synaptic properties is a
ubiquitous theme among neuronal networks.

Acknowledgements

We thank Logan Fickling for help with spike phase analysis. This work funded by
National Science Foundation (IOS: 1755283; DMB) and the Biology Department at
Miami University.

873 **References**

- Doi A, Ramirez J-M. Neuromodulation and the orchestration of the respiratory rhythm. *Respir Physiol Neurobiol* 164: 96–104, 2008. doi: 10.1016/j.resp.2008.06.007.
- Guertin PA. The mammalian central pattern generator for locomotion. *Brain Res Rev* 62: 45–56,
 2009. doi: 10.1016/j.brainresrev.2009.08.002.
- 878 3. **Katz PS**, **Calin-Jageman RJ**. Neuromodulation. *Encyclopedia of Neuroscience*: 497–503, 2009.
- 4. **Marder E**. Neuromodulation of neuronal circuits: Back to the future. *Neuron* 76: 1–11, 2012. doi: 10.1016/j.neuron.2012.09.010.
- Nadim F, Bucher D. Neuromodulation of neurons and synapses. *Curr Opin Neurobiol* 29: 48–56,
 2014. doi: 10.1016/j.conb.2014.05.003.
- 883 6. **Bucher D, Haspel G, Golowasch J, Nadim F**. Central pattern generators. In: *eLS, John Wiley and Sons, Ltd (Ed.).* 2015, p. 1–12.
- Flaive A, Fougère M, van der Zouwen CI, Ryczko D. Serotonergic modulation of locomotor
 activity from basal vertebrates to mammals. Front Neural Circuits 14:590299, 2020. doi:
 10.3389/fncir.2020.590299.
- 888 8. **Blitz DM**. Neural circuit regulation by identified modulatory projection neurons. *Front Neurosci* 17, 2023. doi: 10.3389/fnins.2023.1154769.
- Sillar KT, Simmers J, Combes D. From tadpole to adult frog locomotion. *Curr Opin Neurobiol* 82:
 102753, 2023. doi: 10.1016/j.conb.2023.102753.
- Hooper SL, Moulins M. Cellular and synaptic mechanisms responsible for a long-lasting restructuring of the lobster pyloric network. *J Neurophysiol* 64: 1574, 1990. doi: 10.1152/jn.1990.64.5.1574.
- Weimann JM, Meyrand P, Marder E. Neurons that form multiple pattern generators:
 Identification and multiple activity patterns of gastric/pyloric neurons in the crab stomatogastric system. *J Neurophysiol* 65: 111–122, 1991. doi: 10.1152/jn.1991.65.1.111.
- Meyrand P, Simmers J, Moulins M. Dynamic construction of a neural network from multiple pattern generators in the lobster stomatogastric nervous system. *J Neurosci* 14: 630–644, 1994.
- 900 13. **Dickinson PS**. Interactions among neural networks for behavior. *Curr Opin Neurobiol* 5: 792–798,
 901 1995. doi: 10.1016/0959-4388(95)80108-1.
- 902 14. **Faumont S, Combes D, Meyrand P, Simmers J**. Reconfiguration of multiple motor networks by short- and long-term actions of an identified modulatory neuron. *Eur J Neurosci* 22: 2489–2502, 2005. doi: 10.1111/j.1460-9568.2005.04442.x.
- Tryba AK, Peña F, Lieske SP, Viemari J-C, Thoby-Brisson M, Ramirez J-M. Differential modulation of neural network and pacemaker activity underlying eupnea and sigh-breathing activities. *J Neurophysiol* 99: 2114–2125, 2008. doi: 10.1152/jn.01192.2007.

- 908 16. **Koch H, Garcia AJ, Ramirez J-M**. Network reconfiguration and neuronal plasticity in rhythm-909 generating networks. *Integr Comp Biol* 51: 856–868, 2011. doi: 10.1093/icb/icr099.
- 910 17. **Fahoum S-RH, Blitz DM**. Neuronal switching between single- and dual-network activity via modulation of intrinsic membrane properties. *J Neurosci* 41: 7848–7863, 2021. doi: 10.1101/2021.02.05.429848.
- 912 10.1101/2021.02.05.429848
- 913 18. **Ramirez J-M**, **Baertsch N**. Defining the rhythmogenic elements of mammalian breathing. 914 *Physiology* 33: 302–316, 2018. doi: 10.1152/physiol.00025.2018.
- 915 19. **Falgairolle M, O'Donovan MJ**. V1 interneurons regulate the pattern and frequency of locomotor-916 like activity in the neonatal mouse spinal cord. *PLoS Biol* 17: 1–31, 2019. doi: 917 10.1371/journal.pbio.3000447.
- 918 20. **Rancic V, Gosgnach S**. Recent insights into the rhythmogenic core of the locomotor CPG. *Int J Mol Sci* 22: 1394, 2021. doi: 10.3390/ijms22031394.
- 920 21. Chalif JI, Martinez-Silva M de L, Pagiazitis JG, Murray AJ, Mentis GZ. Control of mammalian
 921 locomotion by ventral spinocerebellar tract neurons. *Cell* 185: 328–344, 2022. doi:
 922 10.1016/j.cell.2021.12.014.
- 923 22. Drion G, Franci A, Sepulchre R. Cellular switches orchestrate rhythmic circuits. *Biol Cybern* 113:
 924 71–82, 2019. doi: 10.1007/s00422-018-0778-6.
- 925 23. Snyder RR, Blitz DM. Multiple intrinsic membrane properties are modulated in a switch from
 926 single- to dual-network activity. *J Neurophysiol* 128: 1181–1198, 2022. doi:
 927 10.1152/jn.00337.2022.
- 928 24. Nusbaum MP, Marder E. A modulatory proctolin-containing neuron (MPN). II. State-dependent
 929 modulation of rhythmic motor activity. *J Neurosci* 9: 1600–1607, 1989. doi: 10.1523/jneurosci.09 930 05-01600.1989.
- 931 25. **Norris BJ, Coleman MJ, Nusbaum MP**. Recruitment of a projection neuron determines gastric 932 mill motor pattern selection in the stomatogastric nervous system of the crab, *Cancer borealis*. *J* 933 *Neurophysiol* 72: 1451–1463, 1994. doi: 10.1152/jn.1994.72.4.1451.
- 934 26. **Norris BJ, Coleman MJ, Nusbaum MP**. Pyloric motor pattern modification by a newly identified projection neuron in the crab stomatogastric nervous system. *J Neurophysiol* 75: 97, 1996. doi: 10.1152/jn.1996.75.1.97.
- 937 27. **Wu AJ, Cohen LB, Falk CX**. Neuronal activity during different behaviors in *Aplysia*: A distributed organization? *Science* 263: 820–823, 1994. doi: 10.1126/science.8303300.
- 939 28. **Nusbaum MP**, **Beenhakker MP**. A small-systems approach to motor pattern generation. *Nature* 417: 343–350, 2002. doi: 10.1038/417343a.
- 941 29. Daur N, Nadim F, Bucher D. The complexity of small circuits: the stomatogastric nervous system.
 942 Curr Opin Neurobiol 41: 1–7, 2016. doi: 10.1016/j.conb.2016.07.005.

- 943 30. **Evans CG**, **Barry MA**, **Jing J**, **Perkins MH**, **Weiss KR**, **Cropper EC**. The complement of projection neurons activated determines the type of feeding motor program in *Aplysia*. *Front Neural Circuits* 15: 685222, 2021. doi: 10.3389/fncir.2021.685222.
- 946 31. **Devineni A V., Scaplen KM**. Neural circuits underlying behavioral flexibility: Insights from *Drosophila. Front Behav Neurosci* 15: 821680, 2022. doi: 10.3389/FNBEH.2021.821680.
- 948 32. **Namiki S, Ros IG, Morrow C, Rowell WJ, Card GM, Korff W, Dickinson MH**. A population of descending neurons that regulates the flight motor of *Drosophila*. *Curr Biol* 32: 1189-1196.e6, 2022. doi: 10.1016/J.CUB.2022.01.008.
- 951 33. **Coleman MJ, Meyrand P, Nusbaum MP**. A switch between two modes of synaptic transmission mediated by presynaptic inhibition. *Nature* 378: 502–505, 1995. doi: 10.1038/378502a0.
- 953 34. Hooper SL. The pyloric pattern of the lobster (*Panulirus interruptus*) stomatogastric ganglion
 954 comprises two phase-maintaining subsets. *J Comput Neurosci* 4: 207–219, 1997. doi:
 955 10.1023/a:1008867702131.
- 956 35. Marder E, Bucher D. Understanding circuit dynamics using the stomatogastric nervous system of
 957 lobsters and crabs. *Annu Rev Physiol* 69: 291–316, 2007. doi:
 958 10.1146/annurev.physiol.69.031905.161516.
- 959 36. **Blitz DM, Christie AE, Cook AP, Dickinson PS, Nusbaum MP**. Similarities and differences in circuit 960 responses to applied Gly¹-SIFamide and peptidergic (Gly¹-SIFamide) neuron stimulation. *J* 961 *Neurophysiol* 121: 950–972, 2019. doi: 10.1152/jn.00567.2018.
- 962 37. **Gutierrez GJ**, **Grashow RG**. *Cancer borealis* stomatogastric nervous system dissection. *JoVE*: 1–5, 2009. doi: 10.3791/1207.
- Hooper SL, Thuma JB, Guschlbauer C, Schmidt J, Büschges A. Cell dialysis by sharp electrodes can
 cause nonphysiological changes in neuron properties. *J Neurophysiol* 114: 1255–1271, 2015. doi: 10.1152/jn.01010.2014.
- 39. Huybrechts J, Nusbaum MP, Bosch L Vanden, Baggerman G, De Loof A, Schoofs L.
 Neuropeptidomic analysis of the brain and thoracic ganglion from the Jonah crab, *Cancer borealis*. *Biochem Biophys Res Commun* 308: 535–544, 2003. doi: 10.1016/S0006-291X(03)01426-870
 8.
- Yasuda-Kamatani Y, Yasuda A. Characteristic expression patterns of allatostatin-like peptide,
 FMRFamide-related peptide, orcokinin, tachykinin-related peptide, and SIFamide in the olfactory
 system of crayfish *Procambarus clarkii*. *J Comp Neurol* 496: 135–147, 2006. doi:
 10.1002/cne.20903.
- 975 41. Dickinson PS, Stemmler EA, Cashman CR, Brennan HR, Dennison B, Huber KE, Peguero B,
 976 Rabacal W, Goiney CC, Smith CM, Towle DW, Christie AE. SIFamide peptides in clawed lobsters
 977 and freshwater crayfish (Crustacea, Decapoda, Astacidea): A combined molecular, mass
 978 spectrometric and electrophysiological investigation. *Gen and Comp Endocrinol* 156: 347–360,
 979 2008. doi: 10.1016/j.ygcen.2008.01.011.

- 980 42. **Bartos M, Manor Y, Nadim F, Marder E, Nusbaum MP**. Coordination of fast and slow rhythmic neuronal circuits. *J Neurosci* 19: 6650–6660, 1999. doi: 10.1523/JNEUROSCI.19-15-06650.1999.
- 982 43. **Bidaut M**. Pharmacological dissection of pyloric network of the lobster stomatogastric ganglion using picrotoxin. *J Neurophysiol* 44: 1089–1101, 1980. doi: 10.1152/jn.1980.44.6.1089.
- 984 44. **Marder E, Eisen JS**. Electrically coupled pacemaker neurons respond differently to same physiological inputs and neurotransmitters. *J Neurophysiol* 51: 1362–1374, 1984. doi: 10.1152/jn.1984.51.6.1362.
- 987 45. **Haddad SA, Marder E**. Circuit robustness to temperature perturbation is altered by neuromodulators. *Neuron* 100: 609-623.e3, 2018. doi: 10.1016/j.neuron.2018.08.035.
- 989 46. **Stein W**. Modulation of stomatogastric rhythms. *J Comp Physiol* 195: 989–1009, 2009. doi: 10.1007/s00359-009-0483-y.
- 991 47. Shruti S, Schulz DJ, Lett KM, Marder E. Electrical coupling and innexin expression in the
 992 stomatogastric ganglion of the crab *Cancer borealis*. *J Neurophysiol* 112: 2946–2958, 2014. doi:
 993 10.1152/jn.00536.2014.
- 994 48. Dickinson PS, Mecsas C, Marder E. Neuropeptide fusion of two motor-pattern generator circuits.
 995 Nature 344: 155–157, 1990. doi: 10.1038/255243a0.
- 996 49. Marder E, Gutierrez GJ, Nusbaum MP. Complicating connectomes: Electrical coupling creates
 997 parallel pathways and degenerate circuit mechanisms. *Dev Neurobiol* 77: 597–609, 2017. doi: 10.1002/dneu.22410.
- 999 50. **Blitz DM**, **White RS**, **Saideman SR**, **Cook A**, **Christie AE**, **Nadim F**, **Nusbaum MP**. A newly identified extrinsic input triggers a distinct gastric mill rhythm via activation of modulatory projection neurons. *J Exp Biol* 211: 1000–1011, 2008. doi: 10.1242/jeb.015222.
- 1002 51. Getting PA, Dekin MS. Mechanisms of pattern generation underlying swimming in *Tritonia*. IV.
 1003 Gating of central pattern generator. *J Neurophysiol* 53: 466–480, 1985. doi:
 1004 10.1152/jn.1985.53.2.466.
- 1005 52. Marder E, Bucher D. Central pattern generators and the control of rhythmic movements. *Curr* 1006 *Biol* 11: 986–996, 2001. doi: 10.1016/S0960-9822(01)00581-4.
- Marder E, Bucher D, Schulz DJ, Taylor AL. Invertebrate central pattern generation moves along.
 Curr Biol 15: 685–699, 2005. doi: 10.1016/j.cub.2005.08.022.
- Katz PS. Evolution of central pattern generators and rhythmic behaviours. *Philosoph Trans* 371:20150057, 2016. doi: 10.1098/rstb.2015.0057.
- Eisen JS, Marder E. Mechanisms underlying pattern generation in lobster stomatogastric ganglion
 as determined by selective inactivation of identified neurons. III. Synaptic connections of
 electrically coupled pyloric neurons. J Neurophysiol 48: 1392–1415, 1982. doi:
 10.1152/jn.1982.48.6.1392.
- 1015 56. **Mamiya A, Manor Y, Nadim F**. Short-term dynamics of a mixed chemical and electrical synapse in a rhythmic network. *J Neurosci* 23: 9557–9564, 2003. doi: 10.1523/jneurosci.23-29-09557.2003.

- Weaver AL, Hooper SL. Relating network synaptic connectivity and network activity in the lobster
 (*Panulirus interruptus*) pyloric network. *J Neurophysiol* 90: 2378–2386, 2003. doi:
 10.1152/jn.00705.2002.
- Thao S, Sheibanie AF, Oh M, Rabbah P, Nadim F. Peptide neuromodulation of synaptic dynamics in an oscillatory network. *J Neurosci* 31: 13991–14004, 2011. doi: 10.1523/JNEUROSCI.3624-11.2011.
- Buch ER, Liew SL, Cohen LG. Plasticity of sensorimotor networks: Multiple overlapping
 mechanisms. *Neuroscientist* 23: 185–196, 2017. doi: 10.1177/1073858416638641.
- 1025 60. **Marder E, Rue MCP**. From the Neuroscience of Individual Variability to Climate Change. *J Neurosci* 41: 10213–10221, 2021. doi: 10.1523/JNEUROSCI.1261-21.2021.
- 1027 61. **Fahoum S-RH**, **Blitz DM**. Parallel peptide actions underlie recruitment and coordination of a dual-1028 network neuron. bioRxiv 12.15.571956, 23023. Doi: 10.1101/2023.12.15.571956
- 1029 62. **DeLong ND, Kirby MS, Blitz DM, Nusbaum MP**. Parallel regulation of a modulator-activated current via distinct dynamics underlies comodulation of motor circuit output. *J Neurosci* 29: 1031 12355–12367, 2009. doi: 10.1523/JNEUROSCI.3079-09.2009.
- 1032 63. **Rodriguez JC, Blitz DM, Nusbaum MP**. Convergent rhythm generation from divergent cellular mechanisms. *J Neurosci* 33: 18047–18064, 2013. doi: 10.1523/JNEUROSCI.3217-13.2013.
- 1034 64. **Saideman SR, Blitz DM, Nusbaum MP**. Convergent motor patterns from divergent circuits. *J Neurosci* 27: 6664–6674, 2007. doi: 10.1523/JNEUROSCI.0315-07.2007.
- Nadim F, Li X, Gray M, Golowasch J. The role of electrical coupling in rhythm generation in small networks. In: *Network Functions and Plasticity: Perspectives from Studying Neuronal Electrical Coupling in Microcircuits*. 2017, p. 51–78.
- 1039 66. **Alcamí P, Pereda AE**. Beyond plasticity: the dynamic impact of electrical synapses on neural circuits. *Nat Rev Neurosci* 20: 253–271, 2019. doi: 10.1038/s41583-019-0133-5.
- 1041 67. **Vaughn MJ**, **Haas JS**. On the diverse functions of electrical synapses. *Front Cell Neurosci* 16, 2022. doi: 10.3389/fncel.2022.910015.
- 1043 68. **Crunelli V, Hughes SW**. The slow (<1 Hz) rhythm of non-REM sleep: a dialogue between three cardinal oscillators. *Nat Neurosci* 13: 9–17, 2010. doi: 10.1038/nn.2445.
- 1045 69. Ramirez J-M, Dashevskiy T, Marlin IA, Baertsch N. Microcircuits in respiratory rhythm
 1046 generation: commonalities with other rhythm generating networks and evolutionary
 1047 perspectives. Curr Opin Neurobiol 41: 53–61, 2016. doi: 10.1016/j.conb.2016.08.003.
- 1048 70. **Loyola S, Hoogland TM, Hoedemaker H, Romano V, Negrello M, De Zeeuw CI**. How inhibitory and excitatory inputs gate output of the inferior olive. *Elife* 12, 2023. doi: 10.7554/eLife.83239.
- Ashhad S, Kam K, Del Negro CA, Feldman JL. Breathing rhythm and pattern and their influence
 on emotion. *Annu Rev Neurosci* 45: 223–247, 2022. doi: 10.1146/annurev-neuro-090121-014424.

- 1052 72. Hooper RM, Tikidji-Hamburyan RA, Canavier CC, Prinz AA. Feedback control of variability in the
 1053 cycle period of a central pattern generator. *J Neurophysiol* 114: 2741–2752, 2015. doi:
 1054 10.1152/jn.00365.2015.
- Shik ML, Severin F V, Orlovsky GN. Control of walking and running by means of electrical
 stimulation of the mesencephalon. *Electroencephalogr Clin Neurophysiol* 26: 549, 1969.
- 74. Marder E, Calabrese RL. Principles of rhythmic motor pattern generation. *Physiol Rev* 76: 687–
 717, 1996. doi: 10.1152/physrev.1996.76.3.687.
- 75. Del Negro CA, Koshiya N, Butera RJ, Smith JC. Persistent sodium current, membrane properties
 and bursting behavior of pre-Bötzinger complex inspiratory neurons in vitro. *J Neurophysiol* 88:
 2242–2250, 2002. doi: 10.1152/jn.00081.2002.
- To 36. **Ghosh M, Pearse DD**. The role of the serotonergic system in locomotor recovery after spinal cord injury. *Front Neural Circuits* 8: 1–14, 2015. doi: 10.3389/fncir.2014.00151.
- Sharma S, Kim LH, Whelan PJ. Towards a connectome of descending commands controlling locomotion. *Curr Opin Physiol* 8: 70–75, 2019. doi: 10.1016/j.cophys.2018.12.005.
- 78. Gosgnach S, Lanuza GM, Butt SJB, Saueressig H, Zhang Y, Velasquez T, Riethmacher D, Callaway
 EM, Kiehn O, Goulding M. V1 spinal neurons regulate the speed of vertebrate locomotor
 outputs. *Nature* 440: 215–219, 2006. doi: 10.1038/nature04545.
- 79. Cui Y, Kam K, Sherman D, Janczewski WA, Zheng Y, Feldman JL. Defining pre-Bötzinger complex
 rhythm- and pattern-generating neural microcircuits in vivo. *Neuron* 91: 602–614, 2016. doi:
 10.1016/j.neuron.2016.07.003.
- 1072 80. Katz P, Kirk M, Govind C. Facilitation and depression at different branches of the same motor
 1073 axon: evidence for presynaptic differences in release. *J Neurosci* 13: 3075–3089, 1993. doi:
 1074 10.1523/JNEUROSCI.13-07-03075.1993.
- Daur N, Bryan AS, Garcia VJ, Bucher D. Short-term synaptic plasticity compensates for variability
 in number of motor neurons at a neuromuscular junction. *J Neurosci* 32: 16007–16017, 2012.
 doi: 10.1523/JNEUROSCI.2584-12.2012.
- 1078 82. Blitz DM, Pritchard AE, Latimer JK, Wakefield AT. Muscles innervated by a single motor neuron
 1079 exhibit divergent synaptic properties on multiple time scales. J Exp Biol 220: 1233, 2017. doi:
 1080 10.1242/jeb.148908.
- 1081 83. Onasch S, Gjorgjieva J. Circuit stability to perturbations reveals hidden variability in the balance
 1082 of intrinsic and synaptic conductances. *J Neurosci* 40: 3186–3202, 2020. doi:
 1083 10.1523/JNEUROSCI.0985-19.2020.
- Stöber TM, Batulin D, Triesch J, Narayanan R, Jedlicka P. Degeneracy in epilepsy: multiple routes to hyperexcitable brain circuits and their repair. *Commun Biol* 6: 479, 2023. doi: 10.1038/s42003-023-04823-0.

- 1087 85. Katz PS, Eigg MH, Harris-Warrick RM. Serotonergic/cholinergic muscle receptor cells in the crab
 1088 stomatogastric nervous system. I. Identification and characterization of the gastropyloric
 1089 receptor cells. J Neurophysiol 62: 558–570, 1989. doi: 10.1152/jn.1989.62.2.558.
- 1090 86. Combes D, Meyrand P, Simmers J. Dynamic restructuring of a rhythmic motor program by a
 1091 single mechanoreceptor neuron in lobster. *J Neurosci* 19: 3620–3628, 1999. doi:
 1092 10.1523/JNEUROSCI.19-09-03620.1999.
- Hedrich UBS, Smarandache CR, Stein W. Differential activation of projection neurons by two
 sensory pathways contributes to motor pattern selection. *J Neurophysiol* 102: 2866–2879, 2009.
 doi: 10.1152/jn.00618.2009.
- 1096 88. Beenhakker MP, DeLong ND, Saideman SR, Nadim F, Nusbaum MP. Proprioceptor regulation of
 1097 motor circuit activity by presynaptic inhibition of a modulatory projection neuron. *J Neurosci* 25:
 1098 8794–8806, 2005. doi: 10.1523/JNEUROSCI.2663-05.2005.
- 1099 89. **Christie AE, Stein W, Quinlan JE, Beenhakker MP, Marder E, Nusbaum MP**. Actions of a histaminergic/peptidergic projection neuron on rhythmic motor patterns in the stomatogastric nervous system of the crab *Cancer borealis*. *J Comp Neurol* 469: 153–169, 2004. doi: 10.1002/CNE.11003.
- White RS, Nusbaum MP. The same core rhythm generator underlies different rhythmic motor
 patterns. *J Neurosci* 31: 11484–11494, 2011. doi: 10.1523/JNEUROSCI.1885-11.2011.
- 1105 91. **Steriade M, Nunez A, Amzica F**. Intracellular analysis of relations between the slow (<1 Hz) 1106 neocortical oscillation and other sleep rhythms of the electroencephalogram. *J Neurosci* 13: 1107 3266–3283, 1993. doi: 10.1523/jneurosci.13-08-03266.1993.
- 1108 92. Rangel LM, Rueckemann JW, Riviere PD, Keefe KR, Porter BS, Heimbuch IS, Budlong CH,
 1109 Eichenbaum H. Rhythmic coordination of hippocampal neurons during associative memory
 1110 processing. Elife 5: 1–24, 2016. doi: 10.7554/eLife.09849.
- Prinz AA, Bucher D, Marder E. Similar network activity from disparate circuit parameters. *Nat Neurosci* 7: 1345–1352, 2004. doi: 10.1038/nn1352.
- 1113 94. Cronin EM, Schneider AC, Nadim F, Bucher D. Modulation by neuropeptides with overlapping
 1114 targets results in functional overlap in oscillatory circuit activation. *J Neurosci*. JN-RM-1201-23,
 1115 2023. doi: 10.1523/JNEUROSCI.1201-23.2023. Epub ahead of print.
- Swensen AM, Marder E. Multiple peptides converge to activate the same voltage-dependent current in a central pattern-generating circuit. *J Neurosci* 20: 6752–6759, 2000. doi: 10.1523/jneurosci.20-18-06752.2000.
- Swensen AM, Marder E. Modulators with convergent cellular actions elicit distinct circuit
 outputs. *J Neurosci* 21: 4050–4058, 2001. doi: 10.1523/jneurosci.21-11-04050.2001.
- 1121 97. Calabrese RL, Norris BJ, Wenning A. The neural control of heartbeat in invertebrates. *Curr Opin Neurobiol* 41: 68–77, 2016. doi: 10.1016/J.CONB.2016.08.004.

1123 1124 1125	98.	Clemens S, Meyrand P, Simmers J. Feeding-induced changes in temporal patterning of muscle activity in the lobster stomatogastric system. <i>Neurosci Lett</i> 254: 65–68, 1998. doi: 10.1016/S0304-3940(98)00511-4.
1126 1127	99.	White RS, Spencer RM, Nusbaum MP, Blitz DM. State-dependent sensorimotor gating in a rhythmic motor system. <i>J Neurophysiol</i> 118: 2806–2818, 2017. doi: 10.1152/jn.00420.2017.
1128 1129	100.	Heinzel HG . Gastric mill activity in the lobster. I. Spontaneous modes of chewing. <i>J Neurophysiol</i> 59: 528–550, 1988. doi: 10.1152/JN.1988.59.2.528.
1130		
1131		
1132		

Figure Legends

1133

1134

1135

1136

1137

1138

1139

1140

1141

1142

1143

1144

1145

1146

1147

1148

1149

1150

1151

1152

1153

1154

1155

Figure 1. The isolated stomatogastric nervous system (STNS), including modulatory projection neuron MCN5, connectivity among the stomatogastric (STG) neurons, and STG gastric mill and pyloric response to bath application of the MCN5 neuropeptide Gly¹-SIFamide. A. The isolated STNS is comprised of the paired commissural ganglia (CoG), oesophageal ganglion (OG), stomatogastric ganglion (STG), and connecting and peripheral nerves. The MCN5 neuron projects from the CoG through the ion, on, and stn to the STG (26). Hashed lines represent where ions and sons were cut to isolate STG neurons (see Materials and Methods). Black circles around nerves indicate Vaseline wells for extracellular recordings. Solid line across stn indicates a Vaseline wall which was made at the stn that extended across the dish to separate the STG and motor nerves from the modulatory CoGs, OG, and ions and sons during Gly¹-SIFamide superfusion (liquid drop). B. Circuit diagram of the STG indicates chemical inhibitory (ball and stick) and electrical (resistor and diode symbols) synapses between pyloric (red), gastric mill (blue), and gastro-pyloric (red/blue circles) neurons. The MCN5 neuron acts on most STG neurons (grey backgrounds), including inhibiting pyloric neurons LP and PY, exciting the pyloric pacemaker ensemble (AB/PD/LPG), activating gastric mill neurons LG, IC, and DG, and switching pyloric-only LPG into dual pyloric/gastric mill timed bursting (17, 26, 36) (reused from 17). C. Left, In baseline conditions with the *ions* and *sons* cut, only the pyloric rhythm is active (*Left*, Saline *lpgn* [LPG] and pdn [PD]). Middle, Bath application of MCN5 neuropeptide Gly¹-SIFamide increases pyloric frequency (increased PD burst frequency), activates the gastric mill

rhythm (*mvn* [IC], *lgn* [LG], *dgn* [DG]), and switches LPG into dual pyloric plus gastric mill-timed bursting. *Right*, In Gly¹-SIFamide, when the LPG neuron is isolated from pyloric-timed input (PDs OFF) and gastric mill-timed input (PTX to block glutamatergic inhibition), LPG generates gastric mill-timed bursting intrinsically (17, 23). Ganglia: CoG, commissural ganglion; OG, oesophageal ganglion; STG, stomatogastric ganglion.

Nerves: *dgn*, dorsal gastric nerve; *ion*, inferior oesophageal nerve; *lgn*, lateral gastric nerve; *lpgn*, lateral posterior gastric nerve; *lvn*, lateral ventricular nerve; *mvn*, medial ventricular nerve; *on*, oesophageal nerve; *pdn*, pyloric dilator nerve; *son*, superior oesophageal nerve; *stn*, stomatogastric nerve; Neurons: AB, anterior burster; AM, anterior median; DG, dorsal gastric; GM, gastric mill; IC, inferior cardiac; Int1, interneuron 1; LG, lateral gastric; LP, lateral pyloric; LPG, lateral posterior gastric; MCN5, modulatory commissural neuron 5; MG, medial gastric; PD, pyloric dilator; PY, pyloric; VD, ventricular dilator.

Figure 2. Shutting off the pyloric rhythm or altering pyloric frequency does not regulate LPG gastric mill-timed (slow) bursting during Gly¹-SIFamide application. *Ai*, LPG slow bursting occurred during Gly¹-SIFamide bath application in the control condition (*left*) and when the pyloric rhythm was turned off (*right*) with hyperpolarizing current injection in the two PD neurons (downward arrowheads). LPG slow burst cycle period (Ai) and burst duration (Aii) during PD neuron activity (PD ON-pre/-post) and hyperpolarization (PD OFF). Aii, n = 10, p > 0.05, One-way repeated measures ANOVA; Aiii, n = 10, p > 0.05, Friedman repeated measures ANOVA On Ranks. *Ci.* Example recordings of extracellular LPG (*lpgn*) and PD (*pdn*) activity are shown during Gly¹-

Gly¹-SIFamide plus picrotoxin (PTX) application at baseline pyloric frequency ($\textbf{\textit{Bi}}$) and during hyperpolarizing current injection into the two PD neurons to slow the pyloric rhythm ($\textbf{\textit{Bii}}$) or depolarizing current injection in the PDs to increase pyloric rhythm speed ($\textbf{\textit{Biii}}$), and a post-control ($\textbf{\textit{Biv}}$) after a series of current injections. LPG slow burst frequency is plotted as a function of pyloric frequency for a series of current injection performed during Gly¹-SIFamide bath application ($\textbf{\textit{C}}$) or during Gly¹-SIFamide plus PTX application ($\textbf{\textit{C}}$). C, r = 0.020, $r^2 = 0.0004$, p = 0.909, n = 4, Pearson Correlation; D, r = 0.098, $r^2 = 0.009$, p = 0.485, n = 8, Pearson Correlation.

Figure 3. Gastric mill network neurons regulated LPG slow bursting in Gly¹-SIFamide.

A. Intracellular (LG, IC, DG) and extracellular (*Ipgn* [LPG], *pdn* [PD]) recordings during Gly¹-SIFamide application, with LG, IC, and DG neurons active (*Ieft*, LG/IC/DG ON) and during injection of hyperpolarizing current (*right*, LG/IC/DG OFF). LPG generates dual bursting activity during hyperpolarization of LG, IC, and DG. **Bi, Bii.** LPG slow burst cycle period (**Bi**) and burst duration (**Bii**) before (ON-pre), during (OFF), and after (ON-post) individual and simultaneous IC, LG, and DG hyperpolarization. n = 10, One-way repeated measures ANOVA, Holm-Sidak *post hoc* analysis, *p < 0.05; **p < 0.01; ***p < 0.001. Data re-analyzed from 17.

Figure 4. LPG regulated gastric mill network neuron activity but was not necessary for gastric mill rhythm generation.

Ai, Aii. Extracellular recordings of LG (*Ign*), IC (*mvn*), DG (*dgn*), and LPG (*Ipgn*) during Gly¹-SIFamide application with LPG Intact (*Ai*) and LPG photoinactivated (*Aii*, LPG Killed). LG, IC, and DG generated a gastric mill rhythm after LPG was photoinactivated (LPG Killed). Blue boxes indicate IC gastric mill-timed bursting with pyloric timing (red arrows) during LPG Intact and LPG Killed (*Ai* and *Aii*, respectively). *B.* Cycle period, burst duration, number of spikes per burst, and firing frequency of LG (n = 12), DG (n = 10), and IC (n = 11) during LPG Intact and LPG Killed. The same parameters were measured for IC pyloric-timed bursts (Pyloric-IC). IC gastric mill-timed (see Methods) and pyloric-timed (see Methods) bursts were analyzed separately. Paired t-test, **p < 0.01; ***p < 0.001.

Figure 5. Categorization of gastric mill rhythm coordination during Gly¹-SIFamide application.

A. Schematics of possible types of coordination between a reference neuron and two network neurons (Neuron 1, Neuron 2). Each colored shaded region indicates one cycle of rhythmic activity with one type of coordination. For example, in "All Coordinated", Neuron 1 and Neuron 2 each have bursts that begin and end within one cycle of the reference neuron (brown shaded region). In some cases, there can be more than one possibility for a type of coordination. For instance, in the "All Uncoordinated" case, Neurons 1 and 2 may have multiple bursts within one Reference Neuron cycle, or Neuron 1 may have multiple bursts while Neuron 2 fires tonically during the Reference

Neuron cycle. See Methods for a complete description of categories. *Bi-Bii*. Example traces of LG (Ign), IC (mvn), DG (dgn), LPG (Ipgn), and PD (pdn) show different types of coordination between these neurons. **Bi.** Different types of coordination occurred within one preparation during the Gly¹-SIFamide-elicited gastric mill rhythm. In the example shown, coordination was determined among LG, IC, DG, and LPG. At the beginning of the example, there were two cycles of "One Neuron Tonic", in which DG fired tonically. After some time (vertical solid line), there was one cycle of "All Coordinated" activity, then one cycle of "One Neuron Silent" followed by another cycle of "All Coordinated activity. In the "One Neuron Silent" cycle, the DG neuron was identified as silent, as more than 10% of its activity was attributed to the cycle prior, and thus associated with that cycle. Bii. Other example traces, each from different preparations, show physiological examples of other coordination categories. *Left*, The coordination category can be different depending on whether LPG is excluded (brown shading, "All Coordinated") or included (dark blue shading, "One Neuron Uncoordinated") in the categorization analysis. In the "All Silent" cycle, the LPG neuron was identified as silent, as more than 10% of its activity was attributed to the cycle prior, and thus associated with that cycle.

1243

1244

1245

1246

1247

1248

1249

1226

1227

1228

1229

1230

1231

1232

1233

1234

1235

1236

1237

1238

1239

1240

1241

1242

Figure 6. Coordination is stable across multiple Gly¹-SlFamide applications and is not altered by photoinactivation.

Stacked bar graphs of percent cycles per gastric mill network categories for LG, IC, LPG, and DG neurons during two consecutive Gly¹-SIFamide applications (SIF App 1 versus SIF App 2, left, n=5), and during Gly¹-SIFamide applications with GM Intact versus GM Killed (right, n=7).

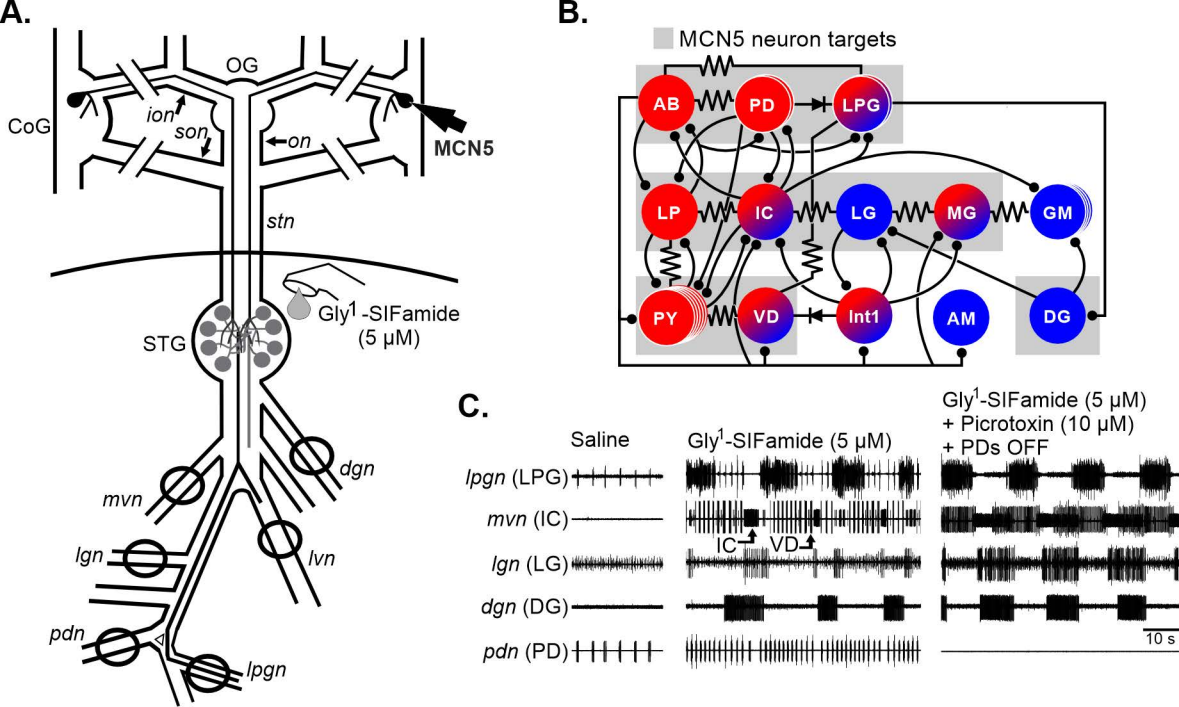
Figure 7. LPG is not necessary for coordinating gastric mill network neuron activity during Gly¹-SlFamide application.

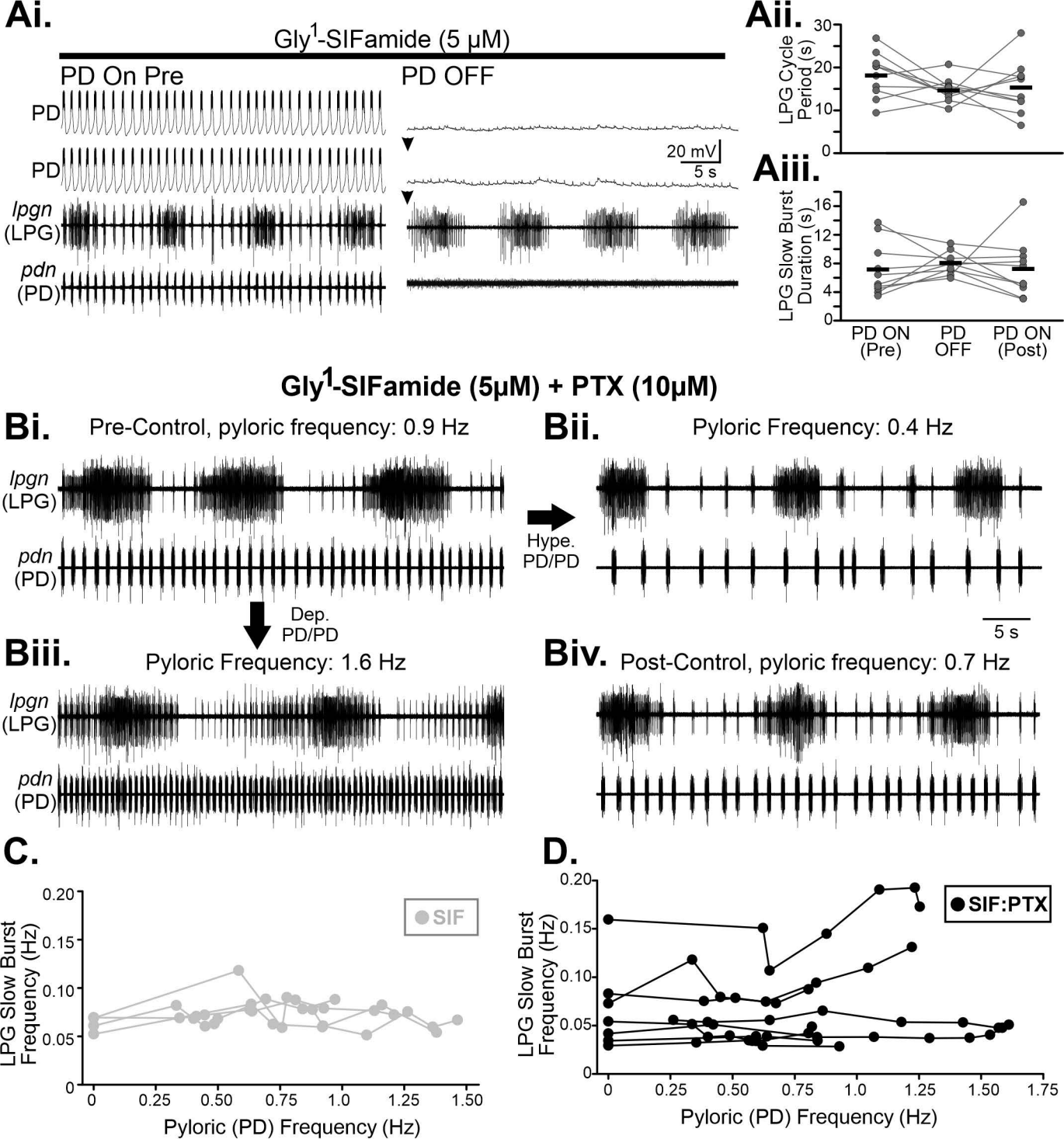
A. Stacked bar graph showing the mean percentage of cyclers per coordination categories for LPG Intact with LPG included in the analysis (LPG Included, n = 9), LPG Intact with LPG excluded from the analysis (LPG Excluded, n = 9), and LPG Killed (n = 10). **Bi-Bii**. Mean percent of gastric mill coordination types for LPG Intact with LPG (LPG Included, n = 9) versus LPG Intact (LPG Excluded, n = 9) (**Bi**) and LPG Intact (LPG Excluded, n = 10) versus LPG Killed (n = 10) (**Bii**). White data points show the percentage of each coordination category from each preparation. Bars indicate mean ± SEM across preparations. **Ci, Cii.** Spike phase analysis of the percent total spikes per bin (100 bins) for LG, IC, DG, and LPG neurons in Gly¹-SIFamide (SIF) LPG Intact (**Ci**) and SIF LPG Killed (**Cii**) conditions. LG is used as a reference neuron. Colored lines for each neuron indicate individual preparations, while the thick black line indicates the mean percent total of spikes per bin across preparations.

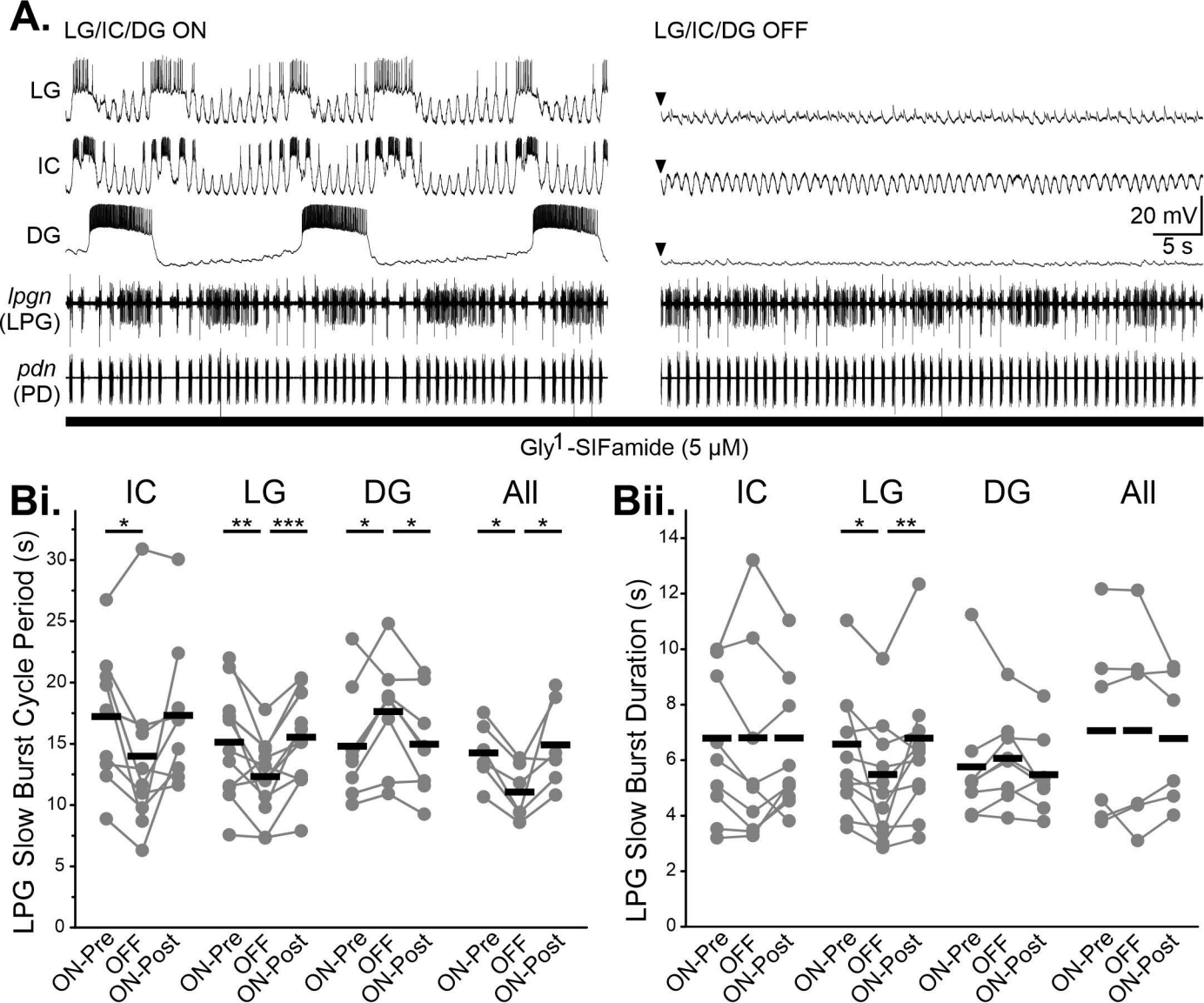
Figure 8. LPG has an active role in mediating coordination among gastric mill network neurons.

A. Example trace recordings of LPG (*lpgn*), LG (*lgn*), IC (*mvn*), and DG (*dgn*) during application of Gly¹-SlFamide with LPG Intact (SlF:LPG Intact, *left*), SlF plus picrotoxin (PTX)with LPG Intact (SlF:PTX:LPG Intact, *middle*), and SlF:PTX:LPG Killed (*right*). During SlF:LPG Intact, there is a triphasic gastric mill rhythm (blue outline), with LPG gastric mill-timed bursting occurring in the second phase (blue filled box). During

SIF:PTX:LPG Intact, glutamatergic inhibitory synapses between LG, IC, and DG are 1273 blocked by PTX, and cholinergic LPG synapses are active. In this condition, LPG 1274 bursting (blue filled box) alternated with LG, IC, and DG bursting (blue outline). In 1275 SIF:PTX:LPG Killed, the gastric mill rhythm was uncoordinated, with tonic LG activity, 1276 irregular IC bursting, and DG bursting activity. Bi, Bii, The mean percentage of 1277 coordination categories are plotted as stacked bars for Gly¹-SIFamide (SIF) LPG Intact 1278 (LPG included) versus SIF:PTX LPG Intact (LPG included) (n = 5) (Bi) and for SIF LPG 1279 Intact (LPG excluded, n = 11) versus SIF:PTX LPG Intact (LPG excluded, n = 5) versus 1280 1281 SIF:PTX LPG Killed (n = 8) (*Bii*). *C.* Spike phase analysis of the percent total of spikes per bin (100 bins) for LG, IC, DG, and LPG neurons in SIF:LPG Intact (left) and 1282 SIF:PTX:LPG Intact (right) conditions. **D.** Spike phase analysis of the percent total of 1283 spikes per bin (100 bins) for LG, IC, DG, and LPG neurons in SIF:LPG Intact (left), 1284 SIF:PTX:LPG Intact (*middle*), and SIF:PTX:LPG Killed (*left*) conditions. 1285 In C and D, LG is used as a reference neuron. Colored lines for each neuron indicate 1286 individual preparations, while the thick black line indicates the mean percent total of 1287 spikes per bin across preparations. 1288







Ai. LPG Intact Ign (LG) VD₃ dgn (DG LPG 10 s Aii. LPG Killed Ign (LG) dgn **Gastric Pyloric** Gastric **Pyloric** LG DG IC IC LG DG IC IC # Spikes/Burst Cycle Period (s) 50 100 50 50 50 16 600 120 40 30 80 40 30 40 40 12 0 00 0 60 30 30 400 80 8 20 10 20 20 20 40 200 40 000 4 10 20 10 10 0 0 0 0 ** Frequency (Hz) 25 20 15 60 50 40 20 12 10 86 4 20 12 10 8 6 4 2 0 6 Burst Dur (s) 3.0 30 16 Firing 12 20 2.0 30 20 10 0 0000 8 10 . 1.0 10 4 5 PC naviled P. P. P. C. Lined PC PC Killed Scotting Tiles P. P. P. C. Tiled P.C. P.C. Villed I PG Intact J. P.G. Killed LPG Intact. 1 P.G. Killed

